

Dalton Transactions

Accepted Manuscript



This is an *Accepted Manuscript*, which has been through the Royal Society of Chemistry peer review process and has been accepted for publication.

Accepted Manuscripts are published online shortly after acceptance, before technical editing, formatting and proof reading. Using this free service, authors can make their results available to the community, in citable form, before we publish the edited article. We will replace this *Accepted Manuscript* with the edited and formatted *Advance Article* as soon as it is available.

You can find more information about *Accepted Manuscripts* in the [Information for Authors](#).

Please note that technical editing may introduce minor changes to the text and/or graphics, which may alter content. The journal's standard [Terms & Conditions](#) and the [Ethical guidelines](#) still apply. In no event shall the Royal Society of Chemistry be held responsible for any errors or omissions in this *Accepted Manuscript* or any consequences arising from the use of any information it contains.

ARTICLE

Influence of *N*-heteroaromatic $\pi\cdots\pi$ stacking on supramolecular assembly and coordination geometry; Effect of single-atom ligand change

Cite this: DOI: 10.1039/x0xx00000x

Received 00th January ????,
Accepted 00th January ????

DOI: 10.1039/x0xx00000x

www.rsc.org/

Hamid Reza Khavasi* and Bahareh Mir Mohammad Sadegh

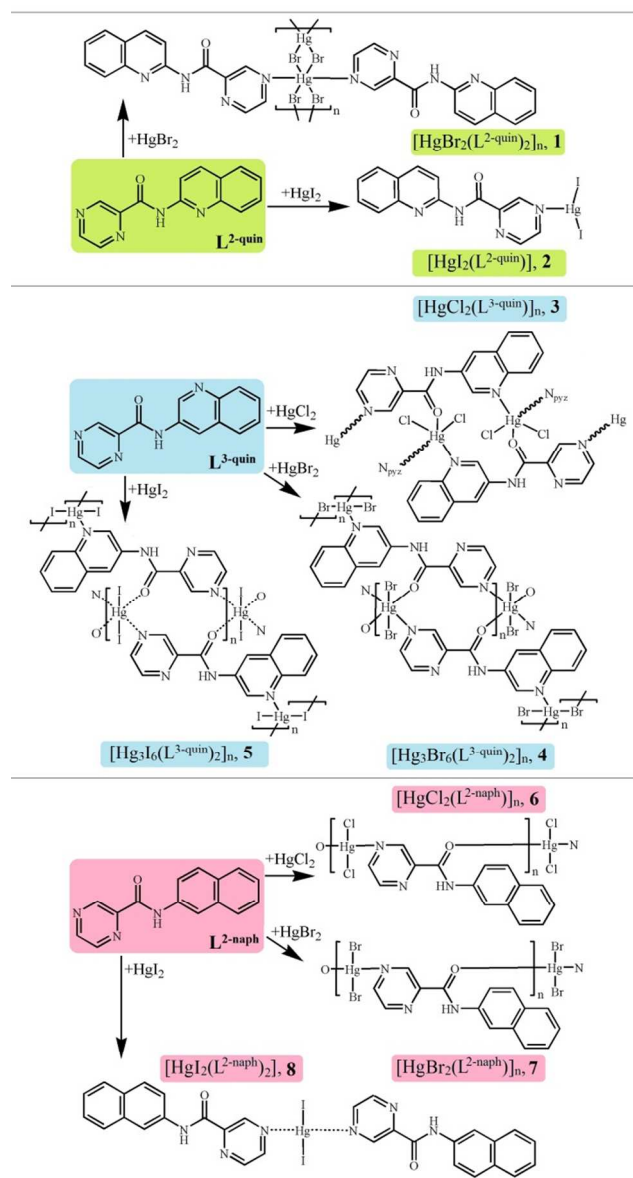
In order to understanding of how the polarization of aromatic systems, through the introducing of nitrogen heteroatom, affects the π - π interactions and crystal packing of mercury coordination compounds, in this study, *N*-(quinolin-2-yl)pyrazine-2-carboxamide and *N*-(quinolin-3-yl)pyrazine-2-carboxamide ligands have been employed for the synthesis of five Hg(II) complexes, $[\text{HgBr}_2(\text{L}^{2\text{-quin}})_2]_n$, **1**, $[\text{HgI}_2(\text{L}^{2\text{-quin}})]$, **2**, $[\text{HgCl}_2(\text{L}^{3\text{-quin}})]_n$, **3**, $[\text{Hg}_3\text{Br}_6(\text{L}^{3\text{-quin}})_2]_n$, **4**, and $[\text{Hg}_3\text{I}_6(\text{L}^{3\text{-quin}})_2]_n$, **5**. X-ray single crystal diffraction analysis of these compounds reveals that all complexes have polymeric structures while complex **2** is a discrete compound. Complexes **1** and **3** have 1D and 2D polymeric structures, respectively, while complexes **4** and **5**, are 3D coordination polymers. In comparison to homologous complexes containing *N*-(naphthalene-2-yl)pyrazine-2-carboxamide ligand, $\text{L}^{2\text{-naph}}$, interestingly, structural analysis clearly shows that the replacement of the naphthyl CH group with a nitrogen atom, changing the spatial extent of the π -electron cloud and polarity of the aromatic ring, from $\text{L}^{2\text{-naph}}$ adducts to $\text{L}^{2\text{-quin}}$ and $\text{L}^{3\text{-quin}}$ adducts, the propensity of the formation of $\pi\cdots\pi$ interactions increases. These π - π stacking interaction synthons affect the coordination geometry and structural assembly. This study reveals an undeniable contribution of π - π stacking interaction to the organization and stabilization of some of the crystal structures reported here.

Introduction

Self-assembly of coordination compounds have been widely studied because their application in materials, catalysis and nanotechnology.¹ This self-assembly and arrangements of molecules of coordination compounds in solids are known to be influenced by a range of directional and non-directional intermolecular interactions. Factors that play an important role in controlling these intermolecular interactions and the architecture of self-assembled species include the ligand structure, which not only provides capability for selective metal ion coordination but can also provide potential interaction sites to generate desired non-covalent interactions,² the metal center,³ counter ions,⁴ and the experimental conditions.⁵ The most extensively exploited of these interactions is highly directional hydrogen bonding.⁶ Other than hydrogen bonding, the influence of $\pi\cdots\pi$ interaction is also well investigated.⁷ It is to be noted that the nature of this interaction is still a matter of dispute. It has been suggested by Martinez and Iverson in 2012,^{7a} that the term " $\pi\cdots\pi$ interaction" does not accurately describe the forces that drive association between aromatic rings. On the other hand, the term " $\pi\cdots\pi$ interaction" appears often to be used generally. This contradiction is due to this fact that there is no important interaction between aromatic π -clouds during face-centered parallel stacking. Instead, off-set stacked geometries are almost observed in aromatics with polarized π -

clouds, such as compounds reported here. Meanwhile, aromatic-aromatic interaction is well accepted among supramolecular chemists⁷ as an important class of intermolecular interactions. Despite this fact, due to the lack of strength and directionality, control of this interaction at the molecular level is difficult. So, one of the key challenges in the understanding of $\pi\cdots\pi$ interaction is investigation of its strength and orientational preferences. In the Hunter and Sanders electrostatic based model, electron donating substituent on the benzene ring increases the repulsion between the two stacked rings, while electron withdrawing substituents should decrease this repulsion.⁸ On the other hand, by considering the non-electrostatic terms such as induction, dispersion and exchange repulsion terms, high-level calculations show that irrespective of the nature of the substituent, presence of all withdrawing and donating groups on benzene ring resulted in the stronger stacking of aromatic ring than unsubstituted benzene.⁹ In this regard, the effect of the replacing the one or more carbon aromatic ring with nitrogen atoms, that resulted in the reduction of the spatial extent of the π -electron clouds and increasing of the polarity of aromatic ring, have also been theoretically investigated in the past few years.¹⁰ Despite to these theoretical studies, experimental investigations on this subject have been relatively rare.¹¹

Although the role of $\pi\cdots\pi$ stacking in metal-containing crystal structures, have been reported, compared to organic systems, to our knowledge, far less attention has been paid to systematic



Scheme 1. Schematic representation of synthetic route of **1-5** and previously published **6-8**.

studies that examine the effect of $\pi \dots \pi$ interactions on the supramolecular aggregation of coordination complexes. Recently, exploiting the $\pi \dots \pi$ stacking capabilities of the π -deficient 1,8-naphthalimide supramolecular synthon,¹² the effect of face-to-face $\pi \dots \pi$ stacking interactions between bipyrimidine ligand in the formation of infinite mercury metal chains^{7d} and the effects of substituent on the geometry of $\pi \dots \pi$ interactions¹³ have been reported. The influence of $\pi \dots \pi$ interactions in the *secondary* structure-directing on the formation of special arrangement have been reported in the literature.¹⁴ Also, study of the $\pi \dots \pi$ stacking effect on the *primary* structure-directing coordination geometry has been reported by us.¹⁵ Due to our interest about $\pi \dots \pi$ interaction effect in the crystal packing of mercury coordination compounds containing pyrazine carboxamide ligands, in 2010, the effect of $\pi \dots \pi$ stacking on the *primary* structure-directing coordination geometry has been discussed by some of us in the structure of Hg(II) complexes containing *N*-(naphthalene-1-yl)pyrazine-2-

carboxamide ligand, L^{1-naph} .^{15c} Recently, in order to further investigate the role of $\pi \dots \pi$ interaction in the crystal packing of coordination compounds, and in comparison to homologous complexes containing *N*-(naphthalene-1-yl)pyrazine-2-carboxamide ligand, L^{1-naph} , we reported the structural analysis of Hg(II) complexes containing *N*-(naphthalene-2-yl)pyrazine-2-carboxamide ligand, L^{2-naph} .^{15a} Presence of strong tendency to form $\pi \dots \pi$ stacking interaction between pyrazine and naphthalene rings is the common feature in the crystal packing of complexes in both groups.

In continuation of our previous studies, here, the crystal structure of Hg(II) complexes of *N*-(quinolin-2-yl)pyrazine-2-carboxamide, L^{2-quin} , and *N*-(quinolin-3-yl)pyrazine-2-carboxamide, L^{3-quin} , ligands, have been analysed. Five Hg(II) complexes of these ligands, $[HgBr_2(L^{2-quin})_2]_n$, **1**, $[HgI_2(L^{2-quin})]_n$, **2**, $[HgCl_2(L^{3-quin})]_n$, **3**, $[Hg_3Br_6(L^{3-quin})_2]_n$, **4**, and $[Hg_3I_6(L^{3-quin})_2]_n$, **5**, have been prepared by the reaction of equimolar quantities of mercury(II) halides (chloride, bromide and iodide) in the mixture of methanol and dimethyl formamide solution for **1** and **2** and in methanolic solution for **3-5**, Scheme 1. Due to the freedom of C-C and C-N single bond rotation in these ligands, the pyrazine and quinoline rings can freely twisted to meet the requirements of the coordination geometries of metal atoms and intermolecular interactions in the assembly process. X-ray diffraction analysis of these complexes and comparison with their similar complexes with L^{1-naph} and L^{2-naph} ligands give details which have led to an understanding of how the polarization of aromatic systems, through the introducing of nitrogen heteroatom, affects the $\pi \dots \pi$ interactions and crystal packing of mercury coordination compounds.

Results and Discussion

Synthesis. The ligands L^{2-quin} and L^{3-quin} was prepared by simply mixing of the same equivalents of quinolin-2-amine or quinolin-3-amine and pyrazinecarboxylic acid in pyridine in the presence of triphenyl phosphite.^{20a} Reaction of equimolar amounts of these ligands and HgX_2 ($X = Cl, Br$ and I) in methanol (for **1** and **2**) and mixture of methanol and dimethyl formamide (for **3-5**) gave the corresponding complexes. Slow evaporation of the solvent resulted in the air-stable yellow needle crystals of **1**, yellow plate crystals of **2**, colorless block crystals of **3**, colorless needle crystals of **4** and yellow prism crystals of **5**, after a few days. It is notable that using 1:1 molar ratio of ligand and HgX_2 in **1**, **4** and **5**, resulted in the same product as when using 1:2 molar ratio for **1** and 3:2 molar ratio for **4** and **5**. Attempts were made to form complexes with $HgCl_2$ using the L^{2-quin} ligand. Yet unfortunately, no mercury-containing suitable crystals for X-ray analysis were isolated from the reaction mixtures during crystal growth. Crystallographic data for compounds **1-5** are listed in Table 1. Selected bond distances and angles are summarized in Table 2.

Structural analysis of HgX_2 complexes with *N*-(quinoline-2-yl)pyrazine-2-carboxamide; $[HgBr_2(L^{2-quin})_2]_n$, **1, and $[HgI_2(L^{2-quin})]_n$, **2**.** The coordination ability of L^{2-naph} was tested with mercury(II) halides. A simple reaction between HgX_2 ($X = Br$ and I) and L^{2-quin} in methanol and DMF at room temperature followed by slow evaporation of the solvent afforded well-formed crystals of $[HgBr_2(L^{2-quin})_2]_n$, **1**, and $[HgI_2(L^{2-quin})]_n$, **2**. X-ray diffraction analysis on a single crystal of these complexes revealed that both of them crystallize in the triclinic crystal system with $P\bar{1}$ space group, Table 1.

The asymmetric unit of $[HgBr_2(L^{2-quin})_2]_n$, **1**, consists of a half crystallographically independent Hg^{2+} ion, one *N*-(quinolin-2-

Table 1. Structural data and refinement for complexes 1-5.

	Complex 1	Complex 2	Complex 3	Complex 4	Complex 5
formula	C ₂₈ H ₂₀ Br ₂ HgN ₈ O ₂	C ₁₄ H ₁₀ HgI ₂ N ₄ O	C ₂₈ H ₂₀ Cl ₄ Hg ₂ N ₈ O ₂	C ₂₈ H ₂₀ Br ₆ Hg ₃ N ₈ O ₂	C ₂₈ H ₂₂ Hg ₃ I ₆ N ₈ O ₂
fw	860.91	704.65	1043.50	1581.69	1863.69
$\lambda/\text{\AA}$	0.71073	0.71073	0.71073	0.71073	0.71073
T/K	298(2)	298(2)	298(2)	298(2)	298(2)
crystal.system	Triclinic	Triclinic	Monoclinic	Monoclinic	Monoclinic
space group	$P\bar{1}$	$P\bar{1}$	$P2_1/n$	$P2_1/c$	$P2_1/c$
$a/\text{\AA}$	3.9332(9)	6.7642(5)	14.5287(5)	7.8761(4)	8.1811(4)
$b/\text{\AA}$	12.278(3)	7.7232(7)	14.0469(3)	7.5061(4)	7.7210(3)
$c/\text{\AA}$	14.441(3)	17.7949(15)	15.7245(5)	29.2866(14)	29.8371(17)
$\alpha/^\circ$	99.278(19)	91.562(7)	90	90	90
$\beta/^\circ$	91.024(18)	93.790(6)	111.798(3)	91.498(4)	93.637(4)
$\gamma/^\circ$	92.56(2)	113.327(6)	90	90	90
$V/\text{\AA}^3$	687.3(3)	850.32(12)	2979.65(15)	1730.80(15)	1880.90(16)
$D_{\text{calc}}/\text{Mg m}^{-3}$	2.080	2.752	2.326	3.035	3.291
Z	1	2	4	2	2
μ/mm^{-1}	8.548	12.687	10.692	20.240	17.176
$F(000)$	410	632	1952	1420	1636
$2\theta/^\circ$	58.32	54.00	58.36	58.40	58.40
$R(\text{int})$	0.0985	0.0982	0.1113	0.1007	0.1162
GOOF	0.994	1.056	1.011	1.107	1.093
$R_1^a(I > 2\sigma(I))$	0.0681	0.0901	0.0574	0.0595	0.0618
$wR_2^b(I > 2\sigma(I))$	0.1405	0.1815	0.1165	0.1024	0.1584
CCDC No.	1015774	1015778	1015768	1015772	1015771

$$^a R_1 = \frac{\sum ||F_o| - |F_c||}{\sum |F_o|}. \quad ^b wR_2 = \frac{[\sum (w(F_o^2 - F_c^2)^2) / \sum w(F_o^2)^2]}{2}^{1/2}.$$

yl)pyrazine-3-carboxamide ligand, $L^{2\text{-quin}}$, and one bromide ion. As depicted in Figure 1a, in this compound, the Hg(II) ion adopts an distorted octahedron coordination geometry

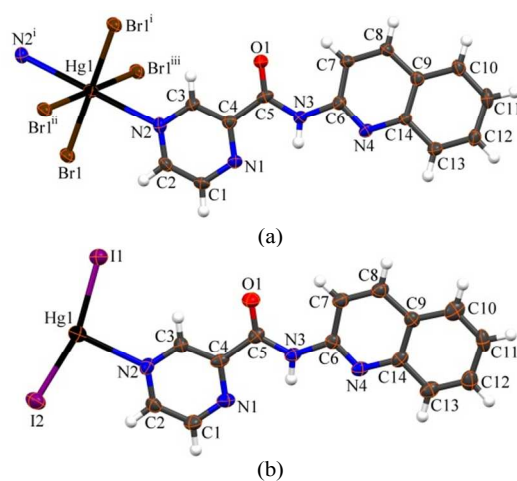


Figure 1. Portion of the structure of coordination compounds formed between $L^{2\text{-quin}}$ and HgBr_2 , **1**, (a), and HgI_2 , **2**, (b), showing coordination geometry around central metal. Symmetry codes: i) 1-x, 1-y, 1-z, ii) -1+x, y, z, iii) 2-x, 1-y, 1-z.

(maximum deviation of angles from 90° is 4.6°) with two nitrogen atoms from $L^{2\text{-quin}}$ ligands and four Br atoms (Hg-Br: 2.487(1) and 3.115(1) \AA), Table 2. Complex **1** is a 1D coordination polymer built up from bromide-bridged Hg(II) edge-sharing octahedral, extending along the a -axis, with a building block of $[\text{HgBr}_2]$, Figure 2a. The Hg...Hg distance within the metal chain is 3.933(9) \AA . This distance is at the upper limit that allows weak mercuriphilic interactions.^{7d,16} Infinite linear mercury chain is further stabilized by intra-chain $\pi \dots \pi$ stacking with ring centroid-to-centroid distances of 3.933 \AA , Table 3. As shown in Figure 2b, overall supramolecular structure results from the linkage of neighbouring coordination polymer chains through head-to-tail $\text{C}_{\text{quin}}\text{-H} \dots \text{O}=\text{C}$ (with the $\text{H} \dots \text{O}$ distance of 2.499(6) \AA) and head-to-tail $\text{C}_{\text{pyz}}\text{-H} \dots \text{N}_{\text{quin}}$ (with the $\text{H} \dots \text{N}_{\text{pyz}}$ distance of 2.780(7) \AA) weak hydrogen bonds. The dihedral angle between pyrazine and quinolin ring is $11.72(18)^\circ$. There is one independent Hg(II) ion, two iodide ions and one $L^{2\text{-quin}}$ ligand in the asymmetric unit of $[\text{HgI}_2(L^{2\text{-quin}})]$, **2**, crystal structure. Figure 1b depicts representative molecular structure showing arrangement about the Hg(II) center for **2** and selected bond distances and angles are listed in Table 2. The Hg(II) atom lies at the center of a distorted T-shape structure defined by two iodide ions (Hg-I: 2.599(1) and 2.602(1) \AA) and one pyrazine nitrogen atom (Hg-N: 2.521(1) \AA) of $L^{2\text{-quin}}$ ligand. For this complex, trigonal-planar index, τ_3 , as defined by some of us,¹⁷ is 0.27, Table 3. As shown in Figure 3a, discrete neutral $[\text{HgI}_2(L^{2\text{-quin}})]$ units stacked on one another

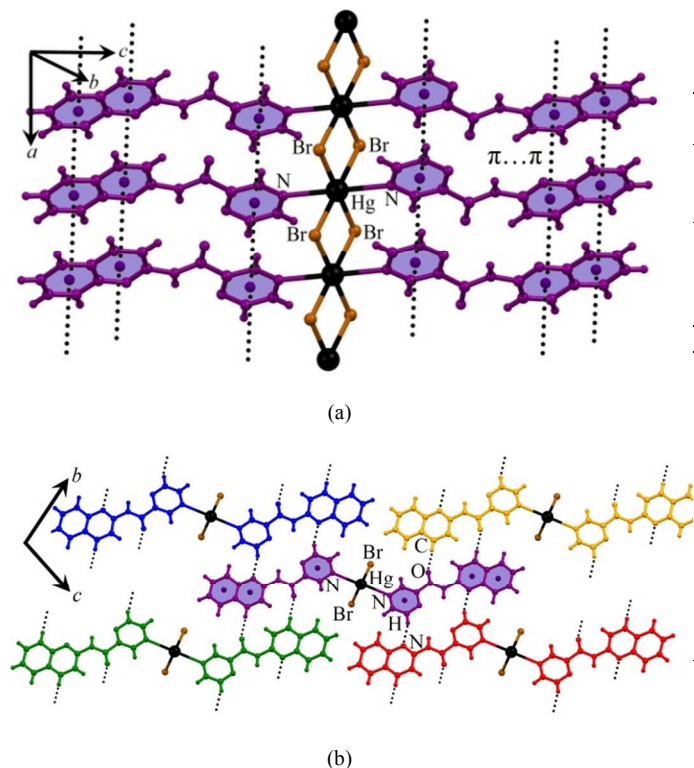


Figure 2. (a) Representation of the 1D linear polymeric chain in **1**, and presence of $\pi \dots \pi$ interaction between adjacent aromatic rings in the chain. (b) A representation of part of **1**, in *a*-direction, showing the formation of overall supramolecular structure from the linkage of neighbouring coordination polymer chains through head-to-tail $C_{\text{quin}}\text{-H}\dots\text{O}=\text{C}$ weak hydrogen bonds and head-to-tail $C_{\text{pyz}}\text{-H}\dots\text{N}_{\text{quin}}$ interactions. Different colours show different adjacent linear chains.

by $\pi \dots \pi$ interaction, with ring centroid-to-centroid distances of 3.736(4) Å, Table 3, in an anti-parallel fashion to form dimeric units. Adjacent dimeric units are further linked to each other to form 2D sheets by cooperation of head-to-tail $C_{\text{quin}}\text{-H}\dots\text{N}_{\text{pyz}}$ (with the $\text{H}\dots\text{N}_{\text{pyz}}$ distance of 2.732(8) Å) and $C_{\text{quin}}\text{-H}\dots\text{O}=\text{C}$ (with the $\text{H}\dots\text{O}$ distance of 2.604(7) Å) weak hydrogen bonds, Figure 3b. In the packing of this complex, the overall supramolecular structure results from the head-to-tail $\text{Hg}\dots\text{I}$ short contacts by distance of 3.932(1) Å, Figure 3c.

Structural analysis of HgX_2 complexes with *N*-(quinoline-3-yl)pyrazine-2-carboxamide; $[\text{HgCl}_2(\text{L}^{3\text{-quin}})]_n$, **3, $[\text{Hg}_3\text{Br}_6(\text{L}^{3\text{-quin}})_2]_n$, **4**, and $[\text{Hg}_3\text{I}_6(\text{L}^{3\text{-quin}})_2]_n$, **5**.** A simple reaction between HgX_2 (X = Cl, Br and I) and $\text{L}^{3\text{-quin}}$ in methanol afforded well-formed crystals of **3-5**. X-ray single crystal diffraction analysis demonstrates that $[\text{HgCl}_2(\text{L}^{3\text{-quin}})]_n$, **3**, crystallizes in the monoclinic crystal system with $P2_1/n$ space group, Table 1. The asymmetric unit of **3**, consists of two crystallographically independent Hg^{2+} ion, four chloride anions and two ligands. As depicted in Figure 4a, according to trigonality index, τ_5 ,¹⁸ of 0.55 and 0.51 for Hg1 and Hg2 atoms, respectively, coordination geometry around the mercury centres can be considered as a highly distorted trigonal bipyramid (TBP), Table 3. In both centers, the basal plane of trigonal bipyramid is occupied by two chloride anions (Hg–Cl: 2.364(2) and 2.348(2) Å), Table 2, and nitrogen atom of quinoline group (Hg–N: 2.380(6) Å), Table 2. The axial positions are occupied by carbonyl oxygen atom (Hg–O: 2.842(7) Å) of $\text{L}^{3\text{-quin}}$ ligand, and a nitrogen atom from the pyrazine ring of the adjacent

Table 2. Selected bond length (Å) and angles (°) around mercury(II) for complexes **1-5**.

		Complex		
		1 (X = Br)	2 (X = I)	
Bond distance	Hg1-X1	2.4870(12), 3.1150(13) ⁱ	2.599(1)	
	Hg1-X2	-	2.602(1)	
	Hg1-N2	2.720(9)	2.521(1)	
Bond angle	X1-Hg1-X1	88.45(4) ⁱ , 180.0 ⁱⁱ	-	
	X1-Hg1-X2	-	163.81(6)	
	N2-Hg1-X1	89.8(2), 94.63(19) ^j	99.5(3)	
	N2-Hg1-X2	-	96.6(3)	
		3 (X = Cl)	4 (X = Br)	5 (X = I)
Bond distance	Hg1-X1	2.364(2)	2.4247(9)	2.5791(12)
	Hg1-X2	2.348(2)	-	-
	Hg1-N2	2.631(6) ⁱⁱⁱ	2.756(1)	2.887(11)
	Hg1-O1	2.842(7)	3.024(3) ^v	3.241(13) ^{ix}
	Hg1-N8	2.380(6)	-	-
	Hg2-X2	-	2.4597(13)	2.642(1)
	Hg2-X3	2.348(2)	3.5181(11), 3.06670(12) ^{vi}	2.7009(8), 3.1182(9) ^x
	Hg2-X4	2.354(2)	-	-
	Hg2-N4	2.393(5)	2.366(7)	2.391(9)
Bond angle	X1-Hg1-X1	-	180.0 ^{viii}	180.0 ^{xi}
	X1-Hg1-X2	143.20(8)	-	-
	N2-Hg1-X1	89.74(16) ⁱⁱⁱ	90.78(11), 89.22(13) ^{vii}	90.46(13), 89.54(11) ^{xii}
	N2-Hg1-X2	92.71(16) ⁱⁱⁱ	-	-
	N2-Hg1-N2	-	180.0 ^{vii}	180.0 ^{xi}
	N8-Hg1-X1	101.42(15)	-	-
	N8-Hg1-X2	114.76(15)	-	-
	N8-Hg1-N2	96.2(2) ⁱⁱⁱ	-	-
	O1-Hg1-X1	90.43(14)	-	-
	O1-Hg1-X2	89.44(13)	-	-
O1-Hg1-N2	176.21(16) ⁱⁱⁱ	101.41(13) ^v , 78.59(12) ^{viii}	104.41(12) ^{ix} , 75.59(11) ^{xii}	
O1-Hg1-N8	80.05(15)	-	-	
X2-Hg2-X3	-	136.80(4), 99.72(4) ^{vi}	130.87(3), 101.60(3) ^x	
X3-Hg2-X3	-	99.81(3) ^{vi}	102.78(2) ^x	
X3-Hg2-X4	145.82(8)	-	-	
X3-Hg2-O2	92.23(14)	-	-	
X2-Hg2-N4	-	106.93(16)	109.50(16)	
X3-Hg2-N4	99.90(15)	111.05(15), 90.43(15) ^{vi}	111.54(16), 1.97(15) ^x	
X3-Hg2-N6	88.42(15) ^{iv}	-	-	
X4-Hg2-O2	89.03(14)	-	-	
X4-Hg2-N4	113.86(15)	-	-	
X4-Hg2-N6	92.60(15) ^{iv}	-	-	
O2-Hg2-N4	79.53(15)	-	-	
O2-Hg2-N6	176.22(15) ^{iv}	-	-	
N4-Hg2-N6	96.7(2) ^{iv}	-	-	

Symmetry codes: (i) $-1+x, y, z$, (ii) $1-x, 1-y, 1-z$, (iii) $1/2-x, -1/2+y, 3/2-z$, (iv) $1/2-x, 1/2+y, 1/2-z$, (v) $1+x, y, z$, (vi) $1-x, -1/2+y, -1/2-z$, (vii) $4-x, 3-y, -z$, (viii) $3-x, 3-y, -z$, (ix) $-1+x, y, z$, (x) $2-x, 1/2+y, 1/2-z$, (xi) $-1-x, 1-y, -z$, (xii) $-x, 1-y, -z$.

ligand at a normal distance of 2.631(6) Å, Table 2. In the crystal packing of this complex, neighboring mercury atoms are linked by the bridging ligand $\text{L}^{3\text{-quin}}$ through the oxygen of the carbonyl group and the nitrogen of the quinoline ring to form a dimeric units, Figure 5a. Overall 2D coordination polymer in *bc*-plane, is formed by linking of mercury atoms of these dimeric units to neighboring metal centres through the pyrazine nitrogen atom of the $\text{L}^{3\text{-quin}}$ ligand, Figure 5b. In the packing of

Table 3. Coordination geometry, dimensionality, C=O-Hg angle and aromatic interaction parameters (\AA and $^\circ$) for description of π - π interaction in $[\text{HgBr}_2(\text{L}^{2\text{-quin}})]_n$, **1**, $[\text{HgI}_2(\text{L}^{2\text{-quin}})]_n$, **2**, $[\text{HgCl}_2(\text{L}^{3\text{-quin}})]_n$, **3**, $[\text{HgBr}_2(\text{L}^{3\text{-quin}})]_n$, **4**, $[\text{HgI}_2(\text{L}^{3\text{-quin}})]_n$, **5**, $[\text{HgCl}_2(\text{L}^{2\text{-naph}})]_n$, **6**, $[\text{HgBr}_2(\text{L}^{2\text{-naph}})]_n$, **7** and $[\text{HgI}_2(\text{L}^{2\text{-naph}})]_2$, **8**.

Complex	Coordination geometry/ dimension	Cg(I)-Cg(J)	Type of π ... π stacking	$d_{\text{Cg-Cg}}^a$	α^b	β, γ^c	$d_{\text{plane-plane}}^d$	d_{offset}^e
$[\text{HgBr}_2(\text{L}^{2\text{-quin}})]_n$, 1	Distorted octahedron /linear chain	Cg(4)-Cg(4) ⁱ	$\pi_{\text{quin-A}} \dots \pi_{\text{quin-A}}$	3.933(4)	0	27.61	3.485(3)	1.82
		Cg(3)-Cg(3) ⁱ	$\pi_{\text{quin-B}} \dots \pi_{\text{quin-B}}$					
		Cg(1)-Cg(1) ⁱ	$\pi_{\text{pyz-P}} \dots \pi_{\text{pyz-P}}$					
$[\text{HgI}_2(\text{L}^{2\text{-quin}})]_n$, 2	T-Shape/discrete	Cg(1)-Cg(3) ⁱⁱ	$\pi_{\text{quin-A}} \dots \pi_{\text{quin-A}}$	3.531(3)	0	11.42	3.462(3)	0.70
		Cg(4)-Cg(4) ⁱ	$\pi_{\text{quin-B}} \dots \pi_{\text{pyz-P}}$	3.736(4)	1.7(7)	24.69, 24.70	3.395(5), 3.395(6)	1.56, 1.56
$[\text{HgCl}_2(\text{L}^{3\text{-quin}})]_n$, 3	TBP/2D sheet	Cg(2)-Cg(4)	$\pi_{\text{quin-A}} \dots \pi_{\text{quin-A}}$	3.649(6)	1.1(4)	17.33, 16.25	3.504(3), 3.484(3)	1.09, 1.02
		Cg(4)-Cg(4) ⁱⁱⁱ	$\pi_{\text{quin-A}} \dots \pi_{\text{quin-A}}$	3.683(6)	0	13.97	3.573(3)	0.89
		Cg(2)-Cg(5) ^{iv}	$\pi_{\text{quin-A}} \dots \pi_{\text{quin-B}}$	3.732(4)	2.4(4)	20.87, 18.53	3.528(3), 3.486(3)	1.33, 1.19
$[\text{HgBr}_2(\text{L}^{3\text{-quin}})]_n$, 4	Distorted octahedron /3D polymer	Cg(1)-Cg(2) ⁱ	$\pi_{\text{quin-A}} \dots \pi_{\text{pyz-P}}$	3.472(5)	1.9(4)	16.00, 14.28	3.365(3), 3.338(4)	0.96, 0.86
		Cg(1)-Cg(3) ⁱ	$\pi_{\text{quin-B}} \dots \pi_{\text{pyz-P}}$	3.682(5)	1.9(4)	24.09, 23.69	3.372(4), 3.361(4)	1.50, 1.48
$[\text{HgI}_2(\text{L}^{3\text{-quin}})]_n$, 5	Distorted octahedron /3D polymer	Cg(1)-Cg(2) ^v	$\pi_{\text{quin-A}} \dots \pi_{\text{pyz-P}}$	3.575(5)	1.5(5)	18.55, 17.91	3.402(4), 3.389(4)	1.14, 1.10
		Cg(1)-Cg(3) ^v	$\pi_{\text{quin-B}} \dots \pi_{\text{pyz-P}}$	3.638(6)	1.8(5)	22.34, 20.78	3.401(6), 3.365(5)	1.38, 1.29
$[\text{HgCl}_2(\text{L}^{2\text{-naph}})]_n$, 6 ^f	Seesaw/linear chain	Cg(1)-Cg(2) ^{vi}	$\pi_{\text{quin-A}} \dots \pi_{\text{pyz-P}}$	3.767(4)	8.3(4)	23.63, 29.10	3.291(3), 3.451(3)	1.83, 1.26
		Cg(1)-Cg(1) ^{vii}	$\pi_{\text{pyz-P}} \dots \pi_{\text{pyz-P}}$	3.702(4)	0	28.59	3.251(3)	1.77
$[\text{HgBr}_2(\text{L}^{2\text{-naph}})]_n$, 7 ^f	Seesaw/linear chain	Cg(1)-Cg(2) ^{vi}	$\pi_{\text{naph-A}} \dots \pi_{\text{pyz-P}}$	3.743(6)	7.8(4)	23.24, 27.39	3.323(4), 3.439(4)	1.88, 1.47
		Cg(3)-Cg(1) ^{viii}	$\pi_{\text{naph-B}} \dots \pi_{\text{pyz-P}}$	3.984(6)	7.6(6)	27.37, 33.63	3.317(4), 3.538(4)	2.20, 1.83
		Cg(1)-Cg(1) ^{viii}	$\pi_{\text{pyz-P}} \dots \pi_{\text{pyz-P}}$	3.786(6)	0	29.61	3.291(4)	1.87
$[\text{HgI}_2(\text{L}^{2\text{-naph}})]_2$, 8 ^f	SP/discrete	Cg(1)-Cg(2) ^{ix}	$\pi_{\text{naph-A}} \dots \pi_{\text{pyz-P}}$	3.695(7)	2.0(6)	24.07, 22.35	3.374(5), 3.418(5)	1.50, 1.40
		Cg(1)-Cg(3) ^{ix}	$\pi_{\text{naph-A}} \dots \pi_{\text{pyz-P}}$	3.520(8)	3.2(6)	17.07, 19.23	3.324(6), 3.365(5)	1.15, 1.03
		Cg(2)-Cg(1) ^{ix}	$\pi_{\text{naph-B}} \dots \pi_{\text{pyz-P}}$	3.820(8)	32.0(6)	24.18, 26.14	3.429(5), 3.485(5)	1.68, 1.56
		Cg(3)-Cg(1) ^{ix}	$\pi_{\text{naph-B}} \dots \pi_{\text{pyz-P}}$	3.847(8)	3.2(6)	23.68, 25.09	3.523(6), 3.484(5)	1.54, 1.63

^a Centroid-centroid distance. ^b Dihedral angle between the ring plane. ^c Offset angles: angle between Cg(I)-Cg(J) vector and normal to plane I, angle between Cg(I)-Cg(J) vector and normal to plane J ($\beta = \gamma$ when $\alpha = 0$). ^d Perpendicular distance of Cg(I) on ring J and perpendicular distance of Cg(J) on ring I. ^e Horizontal displacement between Cg(I) and Cg(J), two values if the two rings are not exactly parallel ($\alpha \neq 0$). ^f From reference 15(a). Colour of the background behind the π ... π interaction values is chosen according to Scheme 4 for better clarity. For **1** and **2**, Cg(1): centroid of N(1)-C(1)-C(2)-N(2)-C(3)-C(4), Cg(3): centroid of C(9)-C(10)-C(11)-C(12)-C(13)-C(14) and Cg(4): centroid of N(4)-C(6)-C(7)-C(8)-C(9)-C(14), For **3**, **4** and **5**, Cg(1): centroid of N(1)-C(1)-C(2)-N(2)-C(3)-C(4), Cg(2): centroid of N(4)-C(7)-C(6)-C(14)-C(13)-C(8), Cg(3): centroid of C(8)-C(9)-C(10)-C(11)-C(12)-C(13), Cg(4): centroid of N(8)-C(21)-C(20)-C(28)-C(27)-C(22) and Cg(5): centroid of C(8)-C(9)-C(10)-C(11)-C(12)-C(13). For **6**, **7** and **8**, Cg(1): centroid of N(1)-C(1)-C(2)-N(2)-C(3)-C(4), Cg(2): centroid of C(6)-C(7)-C(8)-C(13)-C(14)-C(15), Cg(3): centroid of C(8)-C(9)-C(10)-C(11)-C(12)-C(13). Symmetry codes: (i) 1+x, y, z, (ii) 1-x, 2-y, -z, (iii) -x, 2-y, 1-z, (iv) 1-x, 2-y, 1-z, (v) -1+x, y, z, (vi) 1+x, y, z, (vii) 3-x, 1-y, 1-z, (viii) -x, -y, 1-z, (ix) 1/2-x, 1/2+y, 1/2-z.

this complex, the overall supramolecular structure results from the π ... π interactions between adjacent quinoline rings from neighbouring 2D sheets with ring centroid-to-centroid distances of 3.683(6) \AA , Figure 5c, Table 3.

Compounds $[\text{Hg}_3\text{Br}_6(\text{L}^{3\text{-quin}})_2]_n$, **4**, and $[\text{Hg}_3\text{I}_6(\text{L}^{3\text{-quin}})_2]_n$, **5**, consist of two different mercury centers, which have quite different coordination environments. The asymmetric unit of these complexes consist of 1.5 crystallographically independent Hg(II) centers, three halide ions, and one neutral $\text{L}^{3\text{-quin}}$ ligand, Figures 4b and 4c, respectively. So, for these compounds, Table 2 shows three sets of values. In complex **4** the Hg1 atom adopts an distorted octahedron coordination geometry (maximum deviation of angles from 90° is 7.9°) with two nitrogen atoms from $\text{L}^{3\text{-quin}}$ ligands (Hg-N: 2.756(1) \AA), two Br atoms and two oxygen atoms from carbonyl group (Hg-Br: 2.425(1) \AA , Hg-O: 3.024(3) \AA), Table 2.

In **5**, the coordination geometry around the Hg1 atom can be described as a pseudo-six coordinate octahedral with two iodide ions in *trans* position. The four vacant vertexes in the equatorial plane are occupied by two pyrazine nitrogen atoms and two carbonyl oxygen atoms, both in *trans* positions, of four adjacent

$\text{L}^{3\text{-quin}}$ ligands, suggest Hg...N (2.887(11) \AA) and Hg...O (3.241(13) \AA) secondary interactions. Selected bond distances and angles are listed in Table 2. Assuming non-coordinated $\text{L}^{3\text{-quin}}$ ligands in coordination sphere of Hg1, similar to compound **4**, in compound **5**, the coordination geometry can be described as highly distorted octahedron with maximum deviation of 14.4° from 90° . According to four-coordinate geometry index, τ_4 ,¹⁹ of 0.80 and 0.85 for **4** and **5**, respectively, in both compounds, Hg2 atom is in a trigonal pyramidal geometry (TP), coordinated by one nitrogen atom of $\text{L}^{3\text{-quin}}$ ligand and three halide ions.

As shown in Figure 6a, the structure of compounds **4** and **5**, consist of a 1D infinite inorganic chain $[\text{HgX}_2\text{N}]_n$, along *b*-direction. The planar organic ligands stack along both sides of the $[\text{HgX}_2\text{N}]_n$ skeleton and the distance between their mean planes is 7.506 and 7.721 \AA for **4** and **5**, respectively. Each $\text{L}^{3\text{-quin}}$ ligand acts as a bidentate bridging ligand to formation of overall 3D coordination polymer through coordination, in **4**, or secondary bonding interaction, in **5**, to HgX_2 moiety, Figures 6b and 6c, respectively. Figures 6d and 6e also show cooperation of the $\pi_{\text{quin}} \dots \pi_{\text{pyz}}$ interactions with coordination and

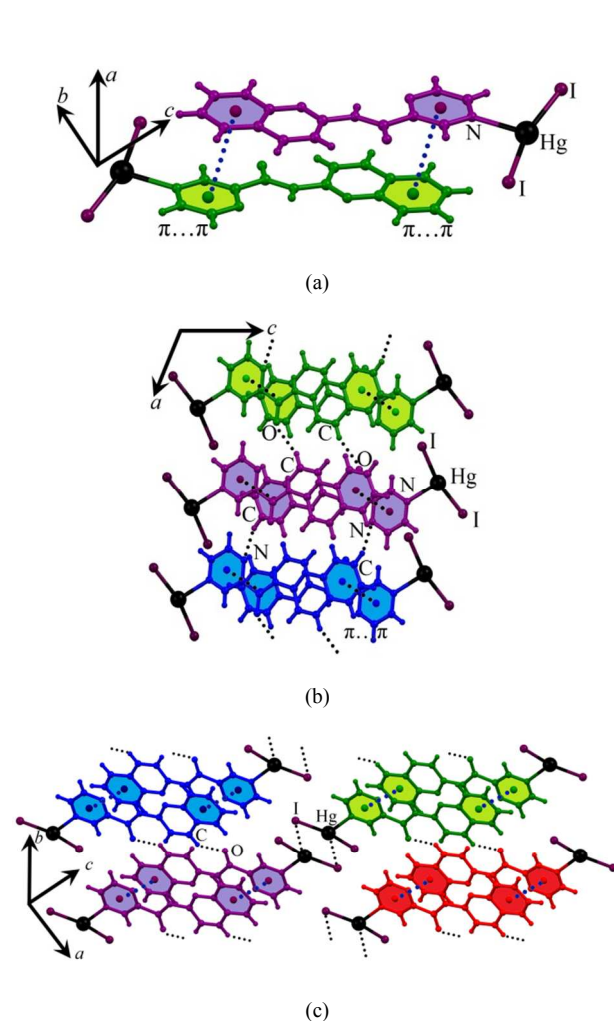


Figure 3. (a) Formation of dimeric units in **2**, through the $\pi \dots \pi$ interaction in an anti-parallel fashion. (b) A side view representation of **2**, in *b*-direction, showing formation of 2D sheets by cooperation of head-to-tail $C_{\text{quin}}\text{-H} \dots N_{\text{pyz}}$ and $C_{\text{quin}}\text{-H} \dots O=C$ weak hydrogen bonding. (c) Formation of overall supramolecular structure in **2**, from the linkage of neighbouring sheets through the head-to-tail Hg...I short contacts.

secondary bondings in the formation of the overall packing of these compounds.

Influence of *N*-heteroaromatic $\pi \dots \pi$ stacking and single-atom ligand change on supramolecular assembly and coordination geometry. Understanding and controlling the structural assemblies of coordination compounds in the solid state requires synthesizing a series of complexes of predetermined chemical structure, allowing for a comparison between resultant supramolecular assemblies with specific and controllable changes to their molecular structure. In this regard, a slight difference in the chemical structure of organic ligand can play an important role in controlling the supramolecular assembly of molecular complexes.^{2b,20} Describing the influence of π - π interactions in the *secondary* structure-directing in the formation of special arrangements has been reported previously.¹⁴ In 2010, the effect π - π stacking on the *primary* structure-directing coordination geometry has been discussed by some of us in the structure of mercury(II) complexes containing *N*-(naphthalene-1-yl)pyrazine-2-carboxamide

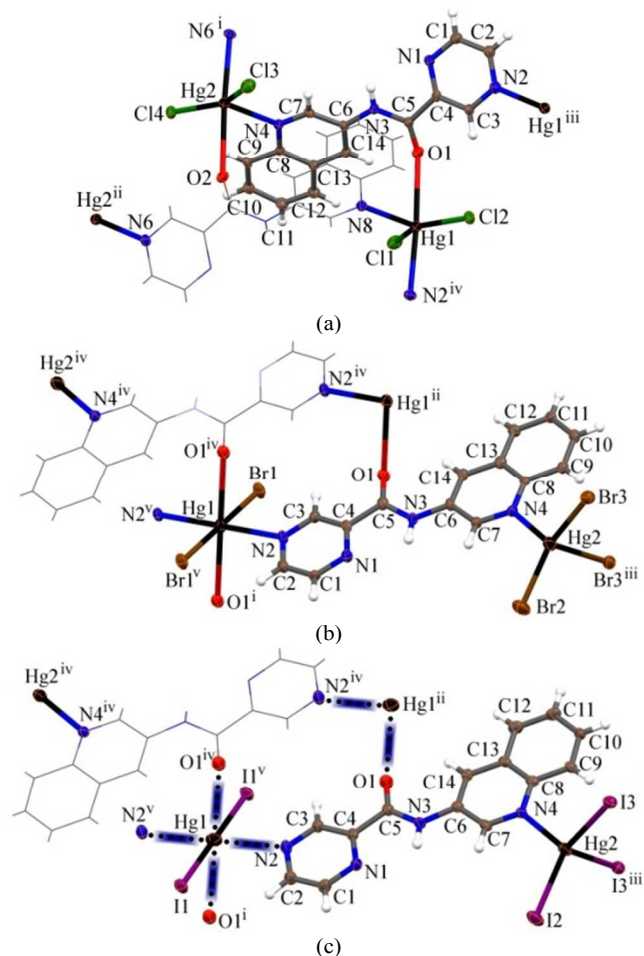


Figure 4. Portion of the structure of coordination compounds formed between $L^{3\text{-quin}}$ and HgCl₂, **3**, (a), HgBr₂, **4**, (b), and HgI₂, **5**, (c), showing coordination geometry around central metal. Secondary bonding is shown in blue. Symmetry codes: (a) i) 1/2-x, 1/2+y, 1/2-z, ii) 1/2-x, -1/2+y, 1/2-z, iii) 1/2-x, 1/2+y, 3/2-z, iv) 1/2-x, -1/2+y, 3/2-z, (b) i) 1+x, y, z, ii) -1+x, y, z, iii) 1-x, -1/2+y, -1/2-z, iv) 3-x, 3-y, -z, v) 4-x, 3-y, -z, (c) i) -1+x, y, z, ii) 1+x, y, z, iii) 2-x, 1/2+y, 1/2-z, iv) -x, 1-y, -z, v) -1-x, 1-y, -z.

ligand, $L^{1\text{-naph}}$ ^{15c} In Our recent report, the effect of position of substituent on the $\pi \dots \pi$ interactions and coordination geometry is investigated. This report shows a systematic studies of π - π stacking synthon on the structural assemblies of Hg(II) complexes of *N*-(naphthalene-2-yl)pyrazine-2-carboxamide ligand, $L^{2\text{-naph}}$ in comparison to homologues complexes containing *N*-(naphthalene-1-yl)pyrazine-2-carboxamide ligand, $L^{1\text{-naph}}$ ^{15a} Interestingly, structural analysis clearly shows that displacing substituent position plays an important role in the formation of the supramolecular organization of molecular complexes. Our investigations clearly showed that compared to the $L^{1\text{-naph}}$ ligand, the displacing substituent position significantly alter the molecular architecture and/or coordination sphere of complexes containing *N*-(naphthalene-2-yl)pyrazine-2-carboxamide ligand, $L^{2\text{-naph}}$. In spite of this, the common feature in the crystal packing of complexes containing both $L^{1\text{-naph}}$ and $L^{2\text{-naph}}$ ligands is the presence of strong tendency to form π - π stacking between adjacent naphthyl and prazine rings in the crystal packing. The polarization of aromatic systems, through the introducing of nitrogen heteroatom, can be affected the π - π interactions and crystal packing of mercury coordination compounds. So, in

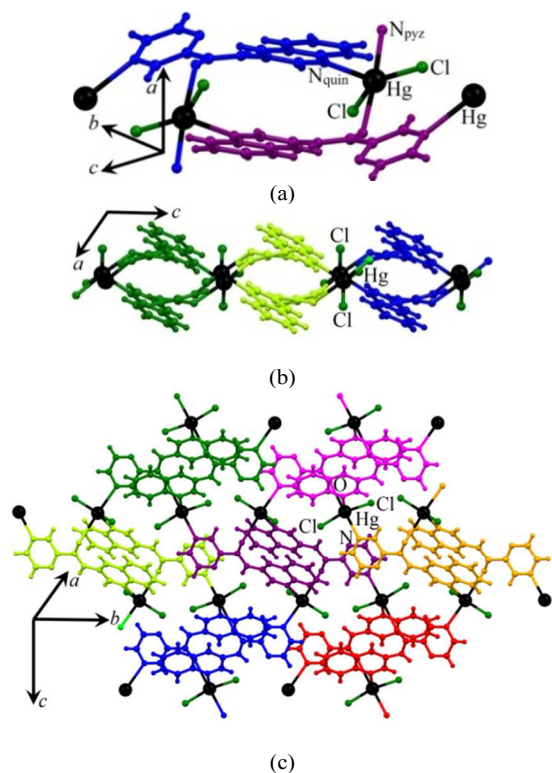


Figure 5. (a) Formation of dimeric units in **3**, through the oxygen of the carbonyl group and the nitrogen of the quinoline ring. (b) Formation of 2D coordination polymer in *ac*-plane by linking of mercury atoms through the pyrazine nitrogen atom. (c) Formation of overall supramolecular structure in **3**, through the $\pi\cdots\pi$ interactions between adjacent quinoline rings from neighbouring 2D sheets.

comparison to homologues complexes containing L^{2-naph} ligands, here, we describe systematic studies of $\pi\cdots\pi$ stacking synthon on the structural assemblies of mercury(II) complexes of *N*-(quinolin-2-yl)pyrazine-2-carboxamide, L^{2-quin} , and *N*-(quinolin-3-yl)pyrazine-2-carboxamide, L^{3-quin} , ligands.

Influence of *N*-heteroaromatic $\pi\cdots\pi$ stacking on supramolecular assembly and coordination geometry.

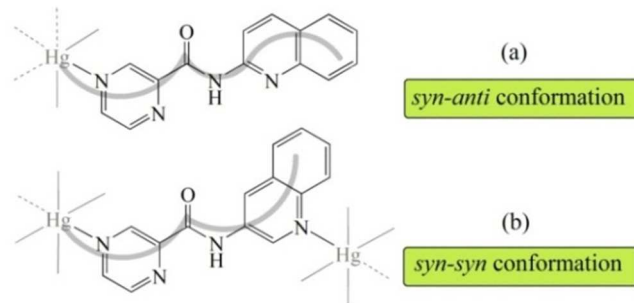
When compared to the L^{2-naph} ligand, the substituting nitrogen for the CH group in the aromatic backbone, significantly alter the molecular architecture and coordination sphere of complexes containing *N*-(quinolin-2-yl)pyrazine-2-carboxamide, L^{2-quin} , and *N*-(quinolin-3-yl)pyrazine-2-carboxamide, L^{3-quin} , ligands. It is notable that the nitrogen atom is isoelectronic with a CH group; thus aromaticity is maintained when CH group constituting the framework of the naphthylpyrazinamide system is replaced by the nitrogen atom. The nitrogen atom of the quinoline ring in the *N*-(quinolinyl)pyrazine-2-carboxamide molecules imports new features into the crystal engineering of mercury(II) coordination compounds containing naphthylpyrazinamide derivatives. The quinolic nitrogen atom either could coordinate to metal center (in HgX_2 adducts with *N*-(quinolin-3-yl)pyrazine-2-carboxamide, L^{3-quin} , ligand) or could affect the $\pi\cdots\pi$ interactions through the changing of the electron distribution of the aromatic ring. It is to be noted, the nitrogen atom of the quinoline ring in L^{2-quin} can probably because of the steric hindrance not coordinate to HgX_2 moiety in **1** and **2**. As listed in Table 3, the coordination geometries and structural motifs in $HgCl_2$ adducts, complexes $[HgCl_2(L^{2-naph})]_n$, **6** and $[HgCl_2(L^{3-}$

Table 4. Selected bond and torsion angles ($^\circ$) in complexes **1-5**.

	Hg-O=C angle	Torsion angle	
		Hg-N _{pyz} -C=O	O=C-C6-C7
$[HgBr_2(L^{2-quin})]_n$, 1	-	19.5(12)	7.9(15)
$[HgI_2(L^{2-quin})]_n$, 2	-	1.6(10)	3.4(16)
$[HgCl_2(L^{2-quin})]_n$, 3	142.1(6)	52.8(7), 50.9(7) ⁱ	149.7(9), 149.1(9) ⁱ
$[HgBr_2(L^{3-quin})]_n$, 4	114.6(9)	12.5(9)	172.2(14)
$[HgI_2(L^{3-quin})]_n$, 5	109.1(8)	12.3(8)	178.9(13)
$[HgCl_2(L^{2-naph})]_n$, 6	130.48(7)	28.7(7)	1.0(7)
$[HgBr_2(L^{2-naph})]_n$, 7	128.67(8)	28.2(8)	1.1(8)
$[HgI_2(L^{2-naph})_2]$, 8	-	5.9(7)	2.6(8)

Symmetry code: (i) 1/2-x, -1/2+y, 3/2-z.

$^{quin})]_n$, **3**, are quite different and 1D linear chain in **6**, with seesaw geometry, is changed to discrete 2D sheet in **3**, with trigonal bipyramid, TBP, geometry. Unfortunately, no mercury-containing suitable crystals for X-ray analysis were isolated from the reaction mixtures of $HgCl_2$ and L^{2-quin} ligand. For $HgBr_2$ adducts, the coordination sphere is Distorted octahedron for $[HgBr_2(L^{2-quin})]_n$, **1**, and $[HgBr_2(L^{3-quin})]_n$, **4**, and seesaw for $[HgBr_2(L^{2-naph})]_n$, **7**. On the other hand, complexes **1** and **7**, have 1D polymeric structures while **4** is a 3D coordination polymer, Table 3. In comparison to the HgI_2 adduct of L^{2-naph} ligand, **8**, that has a square planar geometry, the coordination sphere around central metal in $[HgI_2(L^{2-quin})]_n$, **2**, and $[HgI_2(L^{3-quin})]_n$, **5**, is T-shape and Distorted octahedron, respectively, Table 3. In complexes **2** and **8**, discrete three and four coordinated mercury compounds, respectively, were formed while **5** has a 3D polymeric structure. It is must be noted that, in the HgX_2 adducts of L^{3-quin} ligand, complexes **3-5**, the quinolic nitrogen atom is coordinate to mercury center to generate 2D, in **3**, or 3D, in **4** and **5**, coordination polymers. In spite of this, quinolone rings are also involved in the $\pi\cdots\pi$ interactions with adjacent aromatic rings. In all complexes synthesized here, the pyrazine ring is coordinated to the mercury (II) ion through the N atom *syn* to the carbonyl and the $\pi\cdots\pi$ interactions can be considered as a consequence of this coordination geometry. Meanwhile, the common feature in crystal structures of all eight complexes obtaining of the reaction between HgX_2 and L^{2-quin} , L^{3-quin} and L^{2-naph} ligands, is the existence of $\pi\cdots\pi$ stacking. In these complexes, the dramatic structural changes were clearly resulted from the different conformations adopted by flexible carboxamide ligands. Since the pyrazine and quinoline/naphthyl rings are flexible in rotation around the $C_{pyz}-CON_{amide}$ and $CON_{amide}-C_{quin/naph}$ bonds, this allows for subtle



Scheme 2. *Syn-anti* and *syn-syn* conformations of L^{2-quin} (a) and L^{3-quin} (b) in complexes **1-5**.

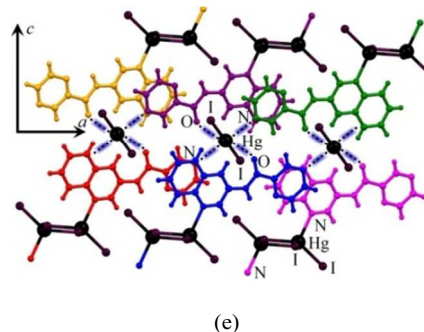
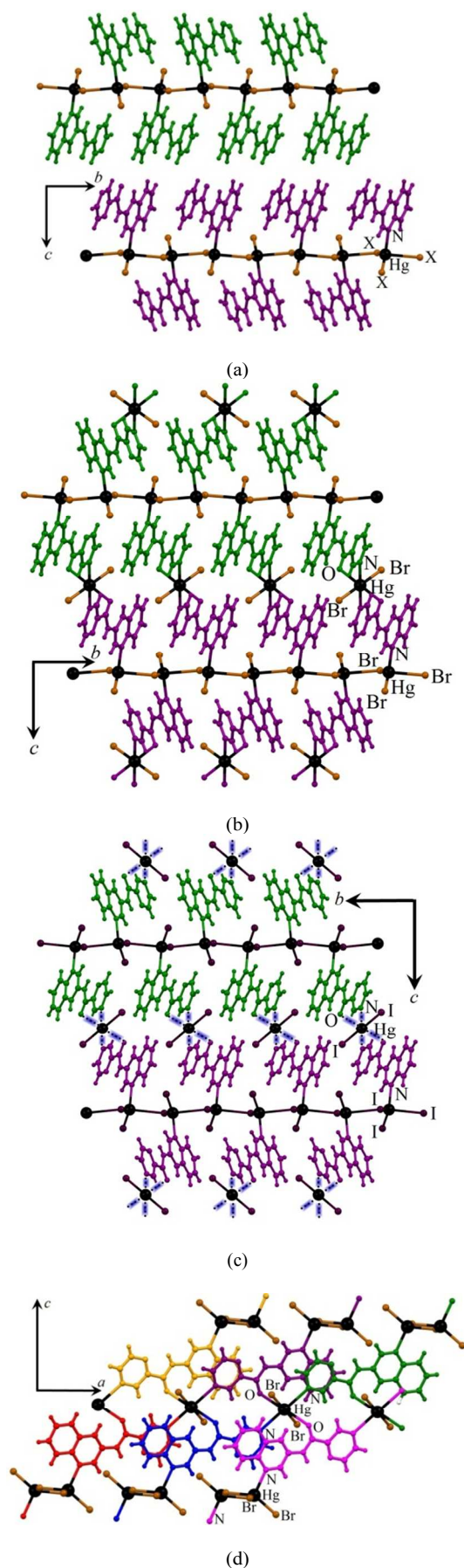


Figure 6. (a) A side view representation of 1D infinite $[\text{HgX}_2\text{N}]_n$ inorganic chains along b -direction in **4** and **5**. Formation of the overall 3D coordination polymers in **4**, (b), and **5**, (c). Cooperation of the $\pi \dots \pi$ interaction with coordination or secondary bonding in the formation of the overall packing of compounds **4**, (d), and **5**, (e), respectively.

conformational adaptation of these ligands to produce $\pi \dots \pi$ interactions *via* the rotation of the rings. Figure 7 shows the $\text{Hg}(\text{X}_2)$ -pyz superimposed pyrazine coordinated units of complexes **1-5**. The conformational variations of the $\text{L}^{2\text{-quin}}$, $\text{L}^{3\text{-quin}}$ and $\text{L}^{2\text{-naph}}$ ligands can be discussed by a dihedral angle of $\text{Hg}-\text{N}_{\text{pyz}}-\text{C}=\text{O}$ and $\text{O}=\text{C}-\text{C}6-\text{C}7$. According to the values listed in Table 4 for these angles, $\text{L}^{2\text{-quin}}$, $\text{L}^{3\text{-quin}}$ and $\text{L}^{2\text{-naph}}$ ligands can be arranged in *syn-anti* conformation in **1**, **2** and **6-8** and *syn-syn* conformation in **3-5**, Scheme 2. In the presence of this flexibility, the quinoline ring can be pointed toward the adjacent aromatic ring to generate $\pi \dots \pi$ stacking synthon. Thus a systematic study evaluation of supramolecular synthons consisting

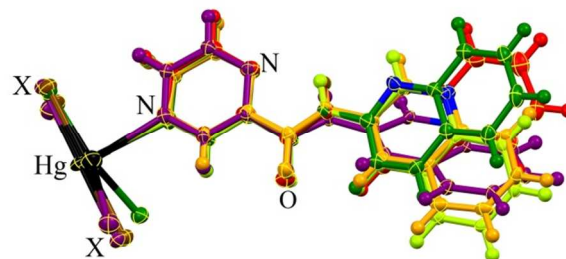
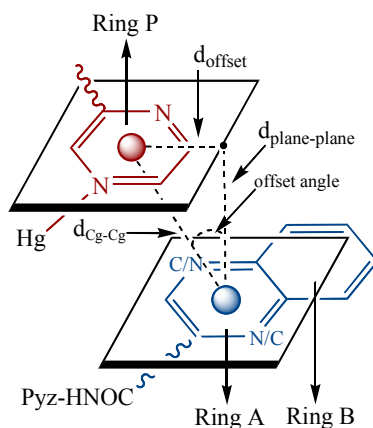


Figure 7. The pyrazine coordinated units of compounds **1** (green), **2** (red), **3** (violet), **4** (light green) and **5** (orange) superimposed to illustrate different conformations and the conformational freedom of the flexible $\text{L}^{2\text{-quin}}$ and $\text{L}^{3\text{-quin}}$ carboxamide ligands.



Scheme 3. Schematic representation of geometrical parameters for definition of $\pi \dots \pi$ stacking between adjacent aromatic rings.

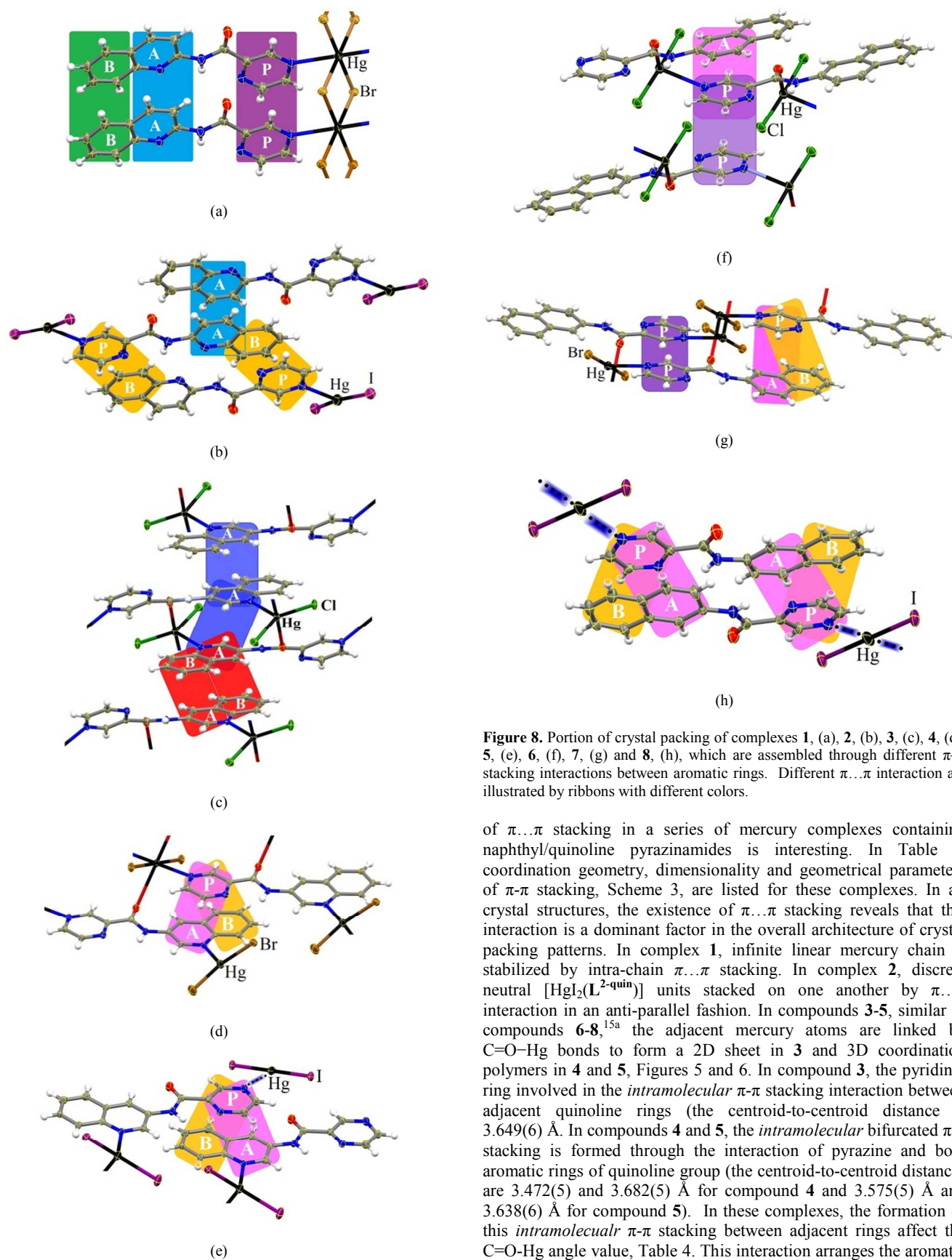


Figure 8. Portion of crystal packing of complexes **1**, (a), **2**, (b), **3**, (c), **4**, (d), **5**, (e), **6**, (f), **7**, (g) and **8**, (h), which are assembled through different π - π stacking interactions between aromatic rings. Different π ... π interaction are illustrated by ribbons with different colors.

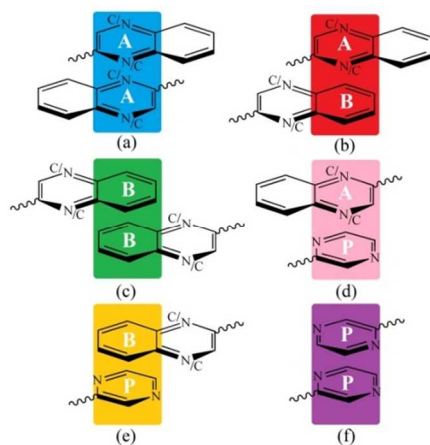
of π ... π stacking in a series of mercury complexes containing naphthyl/quinoline pyrazinamides is interesting. In Table 3, coordination geometry, dimensionality and geometrical parameters of π - π stacking, Scheme 3, are listed for these complexes. In all crystal structures, the existence of π ... π stacking reveals that this interaction is a dominant factor in the overall architecture of crystal packing patterns. In complex **1**, infinite linear mercury chain is stabilized by intra-chain π ... π stacking. In complex **2**, discrete neutral $[\text{HgI}_2(\text{L}^{2\text{-quin}})]$ units stacked on one another by π ... π interaction in an anti-parallel fashion. In compounds **3-5**, similar to compounds **6-8**,^{15a} the adjacent mercury atoms are linked by C=O-Hg bonds to form a 2D sheet in **3** and 3D coordination polymers in **4** and **5**, Figures 5 and 6. In compound **3**, the pyridinyl ring involved in the *intramolecular* π - π stacking interaction between adjacent quinoline rings (the centroid-to-centroid distance is 3.649(6) Å. In compounds **4** and **5**, the *intramolecular* bifurcated π - π stacking is formed through the interaction of pyrazine and both aromatic rings of quinoline group (the centroid-to-centroid distances are 3.472(5) and 3.682(5) Å for compound **4** and 3.575(5) Å and 3.638(6) Å for compound **5**). In these complexes, the formation of this *intramolecular* π - π stacking between adjacent rings affect the C=O-Hg angle value, Table 4. This interaction arranges the aromatic rings in such a way that the angle between the plane normal (involving C-CO-N fragment) and O-Hg vector, θ angle, reaches

about 52.1°, 24.6° and 19.1°, for **3**, **4** and **5**, respectively. These low angles, in comparison to normal range, °, Figure S1, are undoubtedly due to the π - π stacking in the crystal packing of these complexes. The related value for homologous complexes **6** and **7** reported previously by us is 40.5° and 38.7° respectively. A CSD search of θ angle for the geometry of $X_2C=O-Hg$ (X is any atom) shows that the most frequent value for the θ angle is found in the range of 70-90°, Figure S1.²¹ These results confirmed the influence of such π - π stacking synthon on the *primary* structure directing coordination geometry around Hg(II) metal center, that has been reported previously in details by us.^{15c}

Effect of single-atom ligand change on the π ... π stacking and supramolecular architecture.

The π ... π stacking between aromatic rings is extensively investigated.⁷⁻¹⁵ However, its exact nature is still not clearly understood and needs to be further systematic studied at the molecular level. Unlike hydrogen bonding and halogen bond, it is well known that the control of π ... π stacking, as an important interaction in assembling building blocks, is too difficult. This is due to the lack of directionality and strength. Notably, since π ... π stacking is a result of electron delocalization, one can expect different behavior of molecules with different π -electron delocalization. In this regard, theoretical investigations on different series of π -stacked homo- and hetero-dimers, such as pyridine and benzene dimers,^{10a,22} pyridine, pyrazine, 1,3,5-triazine and 1,2,4,5-tetrazine dimers,^{10c} indicate that the introduction of the nitrogen hetero-atom creates a dipole in the molecule and reduces the spatial extent of the π -electron cloud as compared to homo-nuclear one. Although theoretical studies suggest that hetero-atoms play a crucial role in the π ... π stacking, experimental investigations on this subject have been relatively rare.¹¹ A way to studying of the π ... π stacking, experimentally, is considering and analyzing the crystal packing of similar structures.

In similar structures characterized here, complexes **1-8**, and according to orientation of aromatic rings, six types of π ... π stacking can be occurred, Scheme 4. The symbols A and B are referred to the aromatic ring of quinoline or naphthyl connected directly to amidic group and the second ring of them, respectively, while P defines pyrazine ring. So, as example, $\pi_{\text{quin-A}} \dots \pi_{\text{pyz-P}}$ is referred to π ... π interaction between pyrazine ring and the first ring of quinoline



Scheme 4. The various π ... π stacking synthons between aromatic rings, $\pi_{\text{quin/naph-A}} \dots \pi_{\text{quin/naph-A}}$ (a), $\pi_{\text{quin/naph-A}} \dots \pi_{\text{quin/naph-B}}$ (b), $\pi_{\text{quin/naph-B}} \dots \pi_{\text{quin/naph-B}}$ (c), $\pi_{\text{quin/naph-B}} \dots \pi_{\text{pyz-P}}$ (d), $\pi_{\text{pyz-P}} \dots \pi_{\text{pyz-P}}$ (e), and $\pi_{\text{pyz-P}} \dots \pi_{\text{pyz-P}}$ (f), in the crystal packing of complexes **1-8**.

group. Portion of crystal packing of complexes **1-8** which are assembled through different π - π stacking interactions between aromatic rings of adjacent chains are shown in Figure 8. In this figure, different π ... π interaction are illustrated by ribbons with different colors. In Table 2, geometrical parameters of different types of π - π stacking are listed for these complexes. In this Table, color of the background behind each row is chosen according to Scheme 4 for better clarity. As it clear from Table 3 and Figure 8, in HgX_2 adducts with $L^{2\text{-naph}}$ ligand, complexes **6-8**, all π - π stackings including $\pi_{\text{naph-A}} \dots \pi_{\text{pyz-P}}$, $\pi_{\text{naph-B}} \dots \pi_{\text{pyz-P}}$ and $\pi_{\text{pyz-P}} \dots \pi_{\text{pyz-P}}$, are involved with pyrazine π -electron cloud, and no π ... π interaction between naphthyl rings, such as $\pi_{\text{naph-A/B}} \dots \pi_{\text{naph-A/B}}$, is observed. As mentioned above, it has been expected that the replacing the C-H with nitrogen atom increases the polarity and reduces the spatial extent of the π -electron cloud of the quinoline rings in $L^{2\text{-quin}}$ and $L^{3\text{-quin}}$ ligands, as compared to naphthyl ring in $L^{2\text{-naph}}$ ligand. Qualitative support for this replacing in the aromatic backbone and in the solid state organization is provided by a comparison of the electrostatic potential maps for compounds **1-8**, Figure 9. These electrostatic maps show that HgX_2 adducts with $L^{2\text{-quin}}$ and $L^{3\text{-quin}}$, complexes **1-5**, have substantially lower negative electrostatic potentials than HgX_2 adducts with $L^{2\text{-naph}}$, complexes **6-8**, above and below the bicyclic aromatic rings. In our compounds characterized here, it can be concluded that the quinolic nitrogen atom could be the origin of two phenomena: first, an alteration of electron distribution in the bicyclic moiety, in both $L^{2\text{-quin}}$ and $L^{3\text{-quin}}$ adducts; and second, formation of $Hg-N$ coordination mode, in $L^{3\text{-quin}}$ adducts, which affects the π ... π interactions between aromatic rings through the formation of 2D and 3D coordination networks.

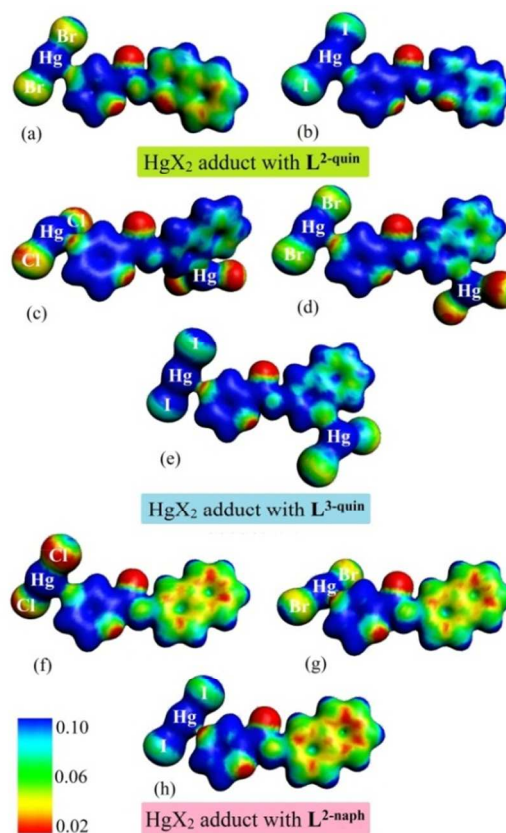


Figure 9. Electrostatic potentials mapped on the electron isodensity surface of compounds **1-8**, (a-h), at the same contour value of 0.02 electron per Bohr³. The computational program renders areas of high electron density as red and low electron density as blue.

In accordance with these, the replacement of the naphthyl CH group with a nitrogen atom and changing the spatial extent of the π -electron cloud and polarity of the aromatic ring, from $L^{2\text{-naph}}$ adducts to $L^{2\text{-quin}}$ and $L^{3\text{-quin}}$ adducts, the propensity of the formation of $\pi\cdots\pi$ interactions increases. So, in complexes **1-3**, $\pi\cdots\pi$ interactions between quinoline π -electron clouds, $\pi_{\text{quin-A}}\cdots\pi_{\text{quin-A}}$ are observed. Compound **1**, is involved with $\pi_{\text{quin-A}}\cdots\pi_{\text{quin-A}}$, $\pi_{\text{quin-B}}\cdots\pi_{\text{quin-B}}$, and $\pi_{\text{pyz-P}}\cdots\pi_{\text{pyz-P}}$ interactions while $\pi_{\text{quin-A}}\cdots\pi_{\text{quin-A}}$ and $\pi_{\text{quin-B}}\cdots\pi_{\text{pyz-P}}$ interactions in complex **2** and $\pi_{\text{quin-A}}\cdots\pi_{\text{quin-A}}$ and $\pi_{\text{quin-A}}\cdots\pi_{\text{quin-B}}$ interactions in complex **3** are main factors in the packing of these compounds. It is notable, according to coordination of quinolic nitrogen atom to mercury ion and formation 3D networks, and due the presence of spatial stress, in **4** and **5**, no $\pi\cdots\pi$ interaction between quinoline rings, such as $\pi_{\text{quin-A/B}}\cdots\pi_{\text{quin-A/B}}$, is observed. In these compounds, $\pi_{\text{quin-A}}\cdots\pi_{\text{pyz-P}}$ and $\pi_{\text{quin-B}}\cdots\pi_{\text{pyz-P}}$ interactions are the main $\pi\cdots\pi$ stackings in the crystal packing of these complexes. It is to be noted that heteroaromatic rings are quite polar; therefore they usually participate in dipolar interactions.²⁸ In the crystal packings containing heteroaromatic rings, alignment of aromatic rings is usually such that the molecular dipoles of contiguous rings are antiparallel or approximately antiparallel.²⁸ This arrangement of heteroaromatic rings is also observed in crystal packing of compounds reported here.

Conclusion

The $\pi\cdots\pi$ stacking interaction synthon can be one of the most powerful non-covalent interactions for directing the self-assembly process of coordination compounds. In this regard, in order to understanding of how the polarization of aromatic systems, through the introducing of nitrogen heteroatom, affects the $\pi\cdots\pi$ interactions and crystal packing of mercury coordination compounds, five Hg(II) complexes containing *N*-(quinolin-2/3-yl)pyrazine-2-carboxamide ligands have been synthesized, characterized and compared with homologues complexes containing *N*-(2-naphthyl)pyrazine-2-carboxamide ligand, previously reported by us. This study clearly shows that the common feature in crystal structures of these complexes is that there is a strong tendency to form $\pi\cdots\pi$ stacking synthon between adjacent aromatic rings. Our results also show that $\pi\cdots\pi$ stacking synthon has the *primary* effect on the coordination geometry of metal center. Interestingly, structural analysis clearly shows that the replacement of the naphthyl CH group with a nitrogen atom and changing the spatial extent of the π -electron cloud, the propensity of the formation of $\pi\cdots\pi$ interactions increases.

Experimental Section

Single crystal diffraction studies. X-ray data for all compounds were collected on STOE IPDS-II or IPDS-2T diffractometer with graphite monochromated Mo-K α radiation. For $[\text{HgBr}_2(L^{2\text{-quin}})_2]_n$, **1**, a yellow needle crystal, for $[\text{HgI}_2(L^{2\text{-quin}})]_n$, **2**, a yellow plate crystal, for $[\text{HgCl}_2(L^{3\text{-quin}})]_n$, **3**, a colorless block crystal, for $[(\text{HgBr}_2)_3(L^{3\text{-quin}})_2]_n$, **4**, a colorless needle crystal and for $[(\text{HgI}_2)_3(L^{3\text{-quin}})_2]_n$, **5**, a yellow prism crystal was chosen using a polarizing microscope and they were mounted on a glass fiber which was used for data collection. Cell constants and an orientation matrix for data collection were obtained by least-squares refinement of diffraction data from 3690 for **1**, 2794 for **2**, 6548 for **3**, 3513 for **4** and 4200 for **5** unique reflections. Data were collected at a temperature of 298(2) K to a maximum θ value of 29.16° for **1**, 27.00° for **2**, 29.18° for **3** and 29.20° for **4** and **5** and in a series of ω scans in 1° oscillations and integrated using the Stöe X-AREA software package.²³ A numerical absorption correction was applied using the X-RED²⁴ and X-SHAPE²⁵ software's. The data were corrected for Lorentz and Polarizing effects. The structures were solved by direct methods²⁶

and subsequent different Fourier maps and then refined on F^2 by a full-matrix least-square procedure using anisotropic displacement parameters. All hydrogen atoms were added at ideal positions and constrained to ride on their parent atoms, with $U_{\text{iso}}(\text{H}) = 1.2U_{\text{eq}}$. All refinements were performed using the X-STEP32 crystallographic software package.²⁷ Structural illustrations have been drawn with MERCURY software.²⁸ Crystallographic data for complexes **1-5** are listed in Table 1. Selected bond distances and angles are summarized in Table 2.

Chemicals and instrumentation. All chemicals were purchased from Aldrich or Merck and used without further purification. The synthesis and recrystallization of *N*-(quinoline-2-yl)pyrazine-2-carboxamide, $L^{2\text{-quin}}$ and *N*-(quinoline-3-yl)pyrazine-2-carboxamide, $L^{3\text{-quin}}$ ligands and compounds **1-5** were carried out in air. Infrared spectra (4000–250 cm^{-1}) of solid samples were taken as 1% dispersions in KBr pellets using a BOMEM-MB102 spectrometer. Elemental analysis was performed using a Heraeus CHN-O Rapid analyzer. ¹H NMR spectrum was recorded on a Bruker AC-300 MHz spectrometer at ambient temperature in DMSO. All chemical shifts are quoted in parts per million (ppm) relative to tetramethylsilane. Melting point was obtained by a Bamstead Electrothermal type 9200 melting point apparatus and corrected.

Synthesis of *N*-(quinoline-2-yl)pyrazine-2-carboxamide, $L^{2\text{-quin}}$ and *N*-(quinoline-3-yl)pyrazine-2-carboxamide, $L^{3\text{-quin}}$. A solution of 5 mmol of α -amino quinoline ($\alpha = 2, 3$) (0.72 g) in 10 mL pyridine was added to a solution of 5 mmol of pyrazine-2-carboxylic acid (0.72 g) in 10 mL pyridine. The resulting solution was stirred at 313 K for 30 min, then 5 mmol of triphenylphosphite (1.3 mL) was added dropwise, and the reaction mixture was stirred at 373 K for 5 h and ambient temperature for 24 h. The resulting yellow solution was added to distilled water, filtered and then washed with 50 mL cold methanol. A light yellow solid resulted with a yield of 70% for $L^{2\text{-quin}}$ and 45% for $L^{3\text{-quin}}$.

Anal. Calcd for $L^{2\text{-quin}}$ ($\text{C}_{14}\text{H}_{10}\text{N}_4\text{O}$): C, 67.19; H, 4.03; N, 22.39. Found: C, 67.21; H, 4.05; N, 22.41. FT-IR (KBr pellet, cm^{-1}): 3354 m, 1690s, 1499 s, 1318 m, 1017 m. ¹H NMR (DMSO, δ from TMS): 10.572 (s, 1H-amidic), 9.362 (s, 1H-pyrazine), 8.985 (s, 1H-pyrazine), 8.847 (s, 1H-pyrazine), 8.419-8.501(m, 2H-quinoline), 7.948, 7.974 (d, 1H-quinoline), 7.854, 7.882 (d, 1H-quinoline), 7.720-7.771 (t, 1H-quinoline), 7.511-7.560 (t, 1H-quinoline).

Anal. Calcd for $L^{3\text{-quin}}$ ($\text{C}_{14}\text{H}_{10}\text{N}_4\text{O}$): C, 67.19; H, 4.03; N, 22.39. Found: C, 67.23; H, 4.07; N, 22.43. FT-IR (KBr pellet, cm^{-1}): 3331 m, 1682s, 1549 s, 1367 w, 1019 m. ¹H NMR (DMSO, δ from TMS): 11.281 (s, 1H-amidic), 9.348, 9.353 (d, 1H-pyrazine), 9.273, 9.281 (d, 1H-pyrazine), 8.967, 8.975 (d, 1H-pyrazine), 8.941, 8.947 (d, 1H-quinoline), 8.853-8.865 (t, 1H-quinoline), 7.964-7.996 (m, 2H-quinoline), 7.658-7.713 (td, 1H-quinoline), 7.574-7.624 (td, 1H-quinoline).

Synthesis of mercury(II) complexes of $L^{2\text{-quin}}$; $[\text{HgBr}_2(L^{2\text{-quin}})_2]_n$, **1, $[\text{HgI}_2(L^{2\text{-quin}})]_n$, **2**.** To a solution of 0.4 mmol of mercury(II) halide (HgX_2 , X = Br and I) in 5 mL of methanol, a solution of 0.4 mmol of *N*-(quinoline-2-yl)pyrazine-2-carboxamide ($L^{2\text{-quin}}$) in 5 mL of methanol was added while stirring. The mixture was heated at 313 K for about 10 min, and resulted sediment. It was then solved by adding 5 mL dimethyl formamide solvent. Upon slow evaporation of this solution at room temperature, yellow needle crystals for $[\text{HgBr}_2(L^{2\text{-quin}})_2]_n$ and yellow plate crystals for $[\text{HgI}_2(L^{2\text{-quin}})]_n$ complexes, suitable for X-ray analysis were obtained after ca. two weeks (yield ca. 72% and 56% for $[\text{HgBr}_2(L^{2\text{-quin}})_2]_n$ and $[\text{HgI}_2(L^{2\text{-quin}})]_n$).

quin)] , respectively). Anal. Calc. for **1** (C₂₈H₂₀Br₂HgN₈O₂): C, 39.06; H, 2.34; N, 13.02. Found: C, 39.10; H, 2.36; N, 13.04. FT-IR (KBr pellet, cm⁻¹): 3343 m, 1693 s, 1596 m, 1013 m, 689 m. Anal. Calc. for **2** (C₁₄H₁₀I₂HgN₄O): C, 23.86; H, 1.43; N, 7.95. Found: C, 23.90; H, 1.48; N, 8.00. FT-IR (KBr pellet, cm⁻¹): 3345 m, 1680 s, 1593 m, 1009 m, 670 m.

Synthesis of mercury(II) complexes of L^{3-quin}; [HgCl₂(L^{3-quin})_n], **3, [(HgBr₂)₃(L^{3-quin})₂]_n, **4**, [(HgI₂)₃(L^{3-quin})₂]_n, **5**.** To a solution of 0.5 mmol of mercury(II) halide (HgX₂, X = Cl, Br and I) in 5 mL of methanol, a solution of 0.5 mmol of N-(quinoline-3-yl)pyrazine-2-carboxamide ligand, L^{3-quin}, in 5 mL methanol was added with stirring. Adding the salt solution resulted to precipitate the complex. By increasing the solvent and temperature of mixture at 313 K for about 15 min, the solution became cleared and then it was filtered. Upon slow evaporation of the filtrate at room temperature, colorless needle crystals for [HgCl₂(L^{3-quin})_n], **3**, colorless needle crystals for [(HgBr₂)₃(L^{3-quin})₂]_n, **4**, and yellow prism crystals for [(HgI₂)₃(L^{3-quin})₂]_n, **5**, suitable for X-ray analysis were obtained after ca. two weeks (yields ca. 52%, 56% and 52% for **3**, **4** and **5**, respectively). Anal. Calc. for **3** (C₁₄H₁₀Cl₂HgN₄O): C, 32.23; H, 1.93; N, 10.74. Found: C, 32.24; H, 1.95; N, 10.77. FT-IR (KBr pellet, cm⁻¹): 3288 m, 1671 s, 1544 s, 1367 m, 876 m, 777 s, 435 s. Anal. Calc. for **4** (C₂₈H₂₀Br₆Hg₃N₈O₂): C, 21.26; H, 1.27; N, 7.08. Found: C, 21.30; H, 1.30; N, 30.33. FT-IR (KBr pellet, cm⁻¹): 3300 m, 1676 s, 1532 s, 1368 m, 876 m, 751 m, 442 m. Anal. Calc. for **5** (C₂₈H₂₀I₆Hg₃N₈O₂): C, 18.04; H, 1.08; N, 6.01. Found: C, 18.07; H, 1.11; N, 32.33. FT-IR (KBr pellet, cm⁻¹): 3293 m, 1676 s, 1528 s, 1362 m, 1013 m, 769 m, 441 m.

ACKNOWLEDGMENT

We would like to thank the Graduate Study Councils of Shahid Beheshti University, General Campus and the Iran National Science Foundation (grant No. 92023015) for financial support.

SUPPORTING INFORMATION

Histogram for the angle (θ, °) between the plane (containing (X)2C=O moiety) normal and Hg-O vector from a CSD search, and X-ray crystallographic files in CIF format for structural determination of **1**, (CCDC No. 1014774), **2**, (CCDC No. 1015778), **3**, (CCDC No. 1015768), **4**, (CCDC No. 1015772), and **5**, (CCDC No. 1015771). This material is free of charge via Internet at <http://pubs.rsc.org>.

- (a) Y. Zhao, Z. Lin, H. Wu and C. Duan, *Inorg. Chem.*, 2006, **45**, 10013; (b) L. C. Tabares, J. A. R. Navarro and J. M. Salas, *J. Am. Chem. Soc.*, 2001, **123**, 383; (c) C. D. Wu, A. G. Hu, L. Zhang and W. B. Lin, *J. Am. Chem. Soc.*, 2005, **127**, 8940; (d) B. Moulton and M. J. Zaworotko, *Chem. Rev.*, 2001, **101**, 1629; (e) S. Kitagawa, R. Kitaura and S. Noro, *Angew. Chem., Int. Ed.*, 2004, **43**, 2334; (f) K. Y. Wang, L. J. Zhou, M. L. Feng and X. Y. Huang, *Dalton Trans.*, 2012, 6689; (g) S. A. Barnett and N. R. Champness, *Coord. Chem. Rev.*, 2003, **246**, 145; (h) C. S. Liu, X. S. Shi, J. R. Li, J. J. Wang and X. H. Bu, *Cryst. Growth Des.*, 2006, **6**, 656; (i) S. G. Telfer and R. Kuroda, *Coord. Chem. Rev.*, 2003, **242**, 33.
- (a) H. R. Khavasi, A. R. Salimi, H. Eshtiahi-Hosseini and M. M. Amini, *CrystEngComm*, 2011, **13**, 3710; (b) H. R. Khavasi, M. Mehdizadeh Barforoush and M. Azizpoor Fard, *CrystEngComm*, 2012, **14**, 7236; (c) B. Notash, N. Safari and H. R. Khavasi, *CrystEngComm*, 2012, **14**, 6788; (d) B. Notash, N. Safari and H. R. Khavasi, *Inorg. Chem.*, 2010, **49**, 11415; (e) G. Mehla, G. Ramon and S. A. Bourne, *CrystEngComm*, 2014, **16**, 8160; (f) G. Nandi and I. Goldberg, *CrystEngComm*, 2014, **16**, 8327; (g) C. Janiak, *Dalton Trans.*, 2000, 3885. (g) P. Bombicz, T. Gruber, C.

Fischer, W. Weber and A. Kálmán, *CrystEngComm*, 2014, **16**, 3646; (h) B. H. Northrop, Y. R. Zheng, K. W. Chi and P. J. Stang, *Acc. Chem. Res.*, 2009, **42**, 1554; (i) C. J. Elsevier, J. Reedijk, P. H. Walton and M. D. Ward, *Dalton Trans.*, 2003, 1869; (j) B. Olenyuk, A. Fechtenkötter and P. J. Stang, *J. Chem. Soc. Dalton Trans.*, 1998, 1707; (k) G. S. Papaefstathiou and L. R. MacGillivray, *Coord. Chem. Rev.*, 2003, **246**, 169; (l) S. Re and S. Nagase, *Chem. Commun.*, 2004, 658; (m) I. Kuzu, I. Krummenacher, J. Meyer, F. Armbruster and F. Breher, *Dalton Trans.*, 2008, 5836.

- (a) J. Yang, B. Wu, F. Zhuge, J. Liang, C. Jia, Y.-Y. Wang, N. Tang, X.-J. Yang and Q.-Z. Shi, *Cryst. Growth Des.*, 2010, **10**, 2331; (b) F. Gandara, M. E. Medina, N. Snecko, E. Gutierrez-Puebla, D. M. Proserpio and M. Angeles Monge, *CrystEngComm*, 2010, **12**, 711; (c) S.-R. Zheng, Q.-Y. Yang, R. Yang, M. Pan, R. Cao and C.-Y. Su, *Cryst. Growth Des.*, 2009, **9**, 2341.
- (a) P. Manna, S. K. Seth, A. Das, J. Hemming, R. Prendergast, M. Helliwell, S. R. Choudhury, A. Frontera and S. Mukhopadhyay, *Inorg. Chem.*, 2012, **51**, 3557; (b) S. Y. Lee, S. Park, H. J. Kim, J. H. Jung and S. S. Lee, *Inorg. Chem.*, 2008, **47**, 1913; (c) B. L. Schottel, H. T. Chifotides, M. Shatruk, A. Chouai, L. M. Perez, J. Bacsa and K. R. Dunbar, *J. Am. Chem. Soc.*, 2006, **128**, 5895; (d) C. S. Campos-Fernandez, B. L. Schottel, H. T. Chifotides, J. K. Bera, J. Bacsa, J. M. Koomen, D. H. Russell and K. R. Dunbar, *J. Am. Chem. Soc.*, 2005, **127**, 12909; (e) H.-P. Zhou, X.-P. Gan, X.-L. Li, Z.-D. Liu, W.-Q. Geng, F.-X. Zhou, W.-Z. Ke, P. Wang, L. Kong, F.-Y. Hao, J.-Y. Wu and Y.-P. Tian, *Cryst. Growth Des.*, 2010, **10**, 1767; (f) H.-P. Zhou, J.-H. Yin, L.-X. Zheng, P. Wang, F.-Y. Hao, W.-Q. Geng, X.-P. Gan, G.-Y. Xu, J.-Y. Wu, Y.-P. Tian, X.-T. Tao, M.-H. Jiang and Y.-H. Kan, *Cryst. Growth Des.*, 2009, **9**, 3789; (g) F. Zeng, J. Ni, Q. Wang, Y. Ding, S. W. Ng, W. Zhu and Y. Xie, *Cryst. Growth Des.*, 2010, **10**, 1611; (h) T. S. B. Baul, S. Kundu, S. Mitra, H. Höpfl, E. R. T. Tiekink and A. Linden, *Dalton Trans.*, 2013, **42**, 1905; (i) J. Chen, S.-H. Wang, Z.-F. Liu, M.-F. Wu, Y. Xiao, F.-K. Zheng, G.-C. Guo and J.-S. Huang, *New J. Chem.*, 2014, **38**, 269; (j) C.-Q. Wan, Y. Zhang, X.-Z. Sun and H.-J. Yan, *CrystEngComm*, 2014, **16**, 2959; (k) G. Yuan, L. Rong, X. Qiao, L. Ma and X. Wei, *CrystEngComm*, 2013, **15**, 7307.
- (a) H. R. Khavasi and B. Mir Mohammad Sadegh, *Inorg. Chem.*, 2010, **49**, 5356; (b) H. R. Khavasi and M. Esmaili, *CrystEngComm*, 2014, **16**, 8479; (c) X.-G. Guo, W.-B. Yang, X.-Y. Wu, Q.-K. Zhang, L. Lin, R. Yu and C.-Z. Lu, *CrystEngComm*, 2013, **15**, 3654; (d) M.-L. Han, X.-H. Chang, X. Feng, L.-F. Ma and L.-Y. Wang, *CrystEngComm*, 2014, **16**, 1687; (e) C.-P. Li and Du, M. *Chem. Commun.*, 2011, **47**, 5958; (f) S. Y. Lee, J. H. Jung, J. J. Vittal and S. S. Lee, *Cryst. Growth Des.*, 2010, **10**, 1033; (g) S. K. Ghosh and S. Kitagawa, *CrystEngComm*, 2008, **10**, 1739; (h) X. Zhu, X.-G. Liu, B.-L. Li and Y. Zhang, *CrystEngComm*, 2009, **11**, 997; (i) Y. B. Go, X. S. Wang, E. V. Anokhina and A. J. Jacobson, *Inorg. Chem.*, 2005, **44**, 8265; (j) S.-L. Li, K. Tan, Y.-Q. Lan, J.-S. Qin, M.-N. Li, D.-Y. Du, H.-Y. Zang and Z.-M. Su, *Cryst. Growth Des.*, 2010, **10**, 1699; (k) S. Lodhia, A. Turner, M. Papadaki, K. D. Demadis and G. B. Hix, *Cryst. Growth Des.*, 2009, **9**, 1811; (l) P.-X. Yin, J. Zhang, Y.-Y. Qin, J.-K. Cheng, Z.-J. Li and Y.-G. Yao, *CrystEngComm*, 2011, **13**, 3536; (m) M. Kondo, Y. Takashima, J. Seo, S. Kitagawa and S. Furukawa, *CrystEngComm*, 2010, **12**, 2350.
- (a) A. Duong, T. Maris and J. D. Wuest, *Inorg. Chem.*, 2011, **50**, 5605; (b) A. Ali, G. Hundal and R. Gupta, *Cryst. Growth Des.*, 2012, **12**, 1308; (c) D. Natale and J. C. Mareque-Rivas, *Chem. Commun.*, 2008, 425; (d) G. R. Desiraju, *J. Chem. Soc. Dalton Trans.*, 2000, 3745; (e) M. Nishio, *CrystEngComm*, 2004, **6**, 130; (f) L. Brammer, *Dalton Trans.*, 2003, 3145; (g) A. O. F. Jones, C. K. Leech, G. J. McIntyre, C. C. Wilson and L. H. Thomas, *CrystEngComm*, 2014, **16**, 8177; (h) N. Qureshi, D. S. Yufit, K. M. Steed, J. A. K. Howard and J. W. Steed, *CrystEngComm*, 2014, **16**, 8413; (i) K. Pandurangan, J. A. Kitchen, T. McCabe and T. Gunnlaugsson, *CrystEngComm*, 2013, **15**, 1421; (j) I. Cvrtila, V. Stilinović and B. Kaitner, *CrystEngComm*, 2013, **15**, 6585.
- (a) C. R. Martinez, B. L. Iverson, *Chem. Sci.*, 2012, **3**, 2191; (b) D. L. Refer, E. Sirianni, J. J. Horger and M. D. Smith, *Cryst.*

- Growth Des.*, 2010, **10**, 386; (c) D. N. Sredojević, Z. D. Tomić and S. D. Zarić, *Cryst. Growth Des.*, 2010, **10**, 3901; (d) J. Y. Wu, H. Y. Hsu, C.-C. Chan, Y.-S. Wen and C. Tsai, *Cryst. Growth Des.*, 2009, **9**, 258; (e) R. F. Semeniuc, T. J. Reamer and M. D. Smith, *New J. Chem.*, 2010, **34**, 439; (f) Q.-L. Ni, X.-F. Jiang, L.-C. Gui, X.-J. Wang, K.-G. Yang and X.-S. Bi, *New J. Chem.*, 2011, **35**, 2471; (g) M. Ahmad, R. Das, J. Mrozinski, A. Bienko, P. Poddar and P. K. Bharadwaj, *CrystEngComm*, 2014, **16**, 8523; (h) G.-G. Hou, H.-J. Zhao, J.-F. Sun, D. Lin, X.-P. Dai, J.-T. Han and H. Zhao, *CrystEngComm*, 2013, **15**, 577; (i) S. M. Walter, M. G. Sarwar, M. G. Chudzinski, E. Herdtweck, A. J. Lough, S. M. Huber and M. S. Taylor, *CrystEngComm*, 2013, **15**, 3097; (j) J. R. Lane, G. C. Saunders and S. J. Webb, *CrystEngComm*, 2013, **15**, 1293; (k) P. Manna, S. K. Seth, M. Mitra, A. Das, N. J. Singh, S. R. Choudhury, T. Kar and S. Mukhopadhyay, *CrystEngComm*, 2013, **15**, 7879.
- 8 (a) C. A. Hunter and J. K. M. Sanders, *J. Am. Chem. Soc.*, 1990, **112**, 5525; (b) C. A. Hunter, *Chem. Soc. Rev.*, 1994, **23**, 101.
- 9 (a) M. O. Sinnokrot and C. D. Sherrill, *J. Am. Chem. Soc.*, 2004, **126**, 7690; (b) M. O. Sinnokrot and C. D. Sherrill, *J. Phys. Chem. A*, 2003, **107**, 8377; (c) S. E. Wheeler and J. W. G. Bloom, *J. Phys. Chem. A*, 2014, **118**, 6133; (d) A. M. Garcia, J. J. Determan and B. G. Janesko, *J. Phys. Chem. A*, 2014, **118**, 3344; (e) S. A. Arnstein and C. D. Sherrill, *Phys. Chem. Chem. Phys.*, 2008, **10**, 2646; (f) A. L. Ringer, M. O. Sinnokrot, R. P. Lively and C. D. Sherrill, *Chem. Eur. J.*, 2006, **12**, 3821.
- 10 (a) S. Tsuzuki, M. Mikami and S. Yamada, *J. Am. Chem. Soc.*, 2007, **129**, 8656; (b) E. G. Hohenstein and C. D. Sherrill, *J. Phys. Chem. A*, 2009, **13**, 878; (c) B. K. Mishra, N. Sathyamurthy, *J. Theor. Comput. Chem.*, 2006, **5**, 609; (d) B. K. Mishra and N. Sathyamurthy, *J. Phys. Chem. A*, 2005, **109**, 6; (e) P. Mingos, S. Loverix, F. D. Proft and P. Geerlings, *J. Phys. Chem. A*, 2004, **108**, 6038; (f) D. Kim, P. Tarakeshwar and K. S. Kim, *J. Phys. Chem. A*, 2004, **108**, 1250.
- 11 (a) G. Pietraperzia, M. Pasquini, N. Schicchieri, G. Piani, M. Becucci, E. Castellucci, M. Biczysko, J. Bloino and V. Barone, *J. Phys. Chem. A*, 2009, **113**, 14343; (b) T. Goly, U. Spoerel and W. Stahl, *Chem. Phys.*, 2002, **283**, 289; (c) C. A. Haynam, D. V. Brumbaugh and D. H. Levy, *J. Chem. Phys.*, 1983, **79**, 1581; (d) J. Wanna, J. A. Menapace and E. R. Bernstein, *J. Chem. Phys.*, 1986, **85**, 777.
- 12 (a) D. L. Reger, A. Debreczeni and M. D. Smith, *Inorg. Chem.*, 2012, **51**, 1068; (b) D. L. Reger, A. Debreczeni, J. J. Horger and M. D. Smith, *Cryst. Growth Des.*, 2011, **11**, 4068; (c) D. L. Reger, A. Debreczeni and M. D. Smith, *Eur. J. Inorg. Chem.*, 2012, **4**, 712; (d) D. L. Reger, A. Debreczeni and M. D. Smith, *Inorg. Chem.*, 2011, **50**, 11754; (e) D. L. Reger, J. J. Horger and M. D. Smith, *Chem. Commun.*, 2011, **47**, 2805; (f) D. L. Reger, J. J. Horger, A. Debreczeni and M. D. Smith, *Inorg. Chem.*, 2011, **50**, 10225; (g) D. L. Reger, J. J. Horger, M. D. Smith, G. J. Long and F. Grandjean, *Inorg. Chem.*, 2010, **50**, 686.
- 13 S. E. Snyder, B.-S. Huang, Y. W. Chu, H.-S. Lin and J. R. Carey, *Chem. Eur. J.*, 2012, **18**, 12663.
- 14 (a) V. Blanco, D. Abella, E. Pia, C. Platas-Iglesias, C. Peinador and J.M. Quintela, *Inorg. Chem.*, 2009, **48**, 4098; (b) S.-Y. Yang, P. Naumov and S. Fukuzumi, *J. Am. Chem. Soc.*, 2009, **131**, 7247; (c) H. Kumagai, M. Akita-Tanaka, S. Kawata, K. Inoue, C. J. Kepert and M. Kurmoo, *Cryst. Growth Des.*, 2009, **9**, 2734; (d) S. Banerjee, N. N. Adarsh and P. Dastidar, *CrystEngComm*, 2009, **11**, 746.
- 15 (a) H. R. Khavasi and B. Mir Mohammad Sadegh, *Dalton Trans.*, 2014, **43**, 5564; (b) H. R. Khavasi and B. Mir Mohammad Sadegh, *Cryst. Growth Des.*, 2012, **12**, 4798; (c) H. R. Khavasi and M. Azizpoor Fard, *Cryst. Growth Des.*, 2010, **10**, 1892.
- 16 (a) J. B. King, M. R. Haneline, M. Tsunoda and F. P. Gabbai, *J. Am. Chem. Soc.*, 2002, **124**, 9350; (b) P. Pykkö, *Chem. Rev.*, 1997, **97**, 597.
- 17 H. R. Khavasi and A. Azhdari Tehrani, *Inorg. Chem.*, 2013, **52**, 2891.
- 18 A. W. Addison, T. N. Rao, J. Reedijk, J. Van Rijn and G. C. Verschoor, *J. Chem. Soc. Dalton Trans.*, 1984, 1349.
- 19 L. Yang, D. R. Powell and R. P. Houser, *Dalton Trans.*, 2007, 955.
- 20 (a) H. R. Khavasi and A. Azhdari Tehrani, *CrystEngComm*, 2013, **15**, 3222; (b) A. Rodríguez-Dieguez, A. J. Mota, J. M. Seco, M. A. Palacios, A. Romerosa and E. Colacio, *Dalton Trans.*, 2009, 9578; (c) T. Burchell and R. J. Puddappatt, *Inorg. Chem.*, 2005, **44**, 3718; (d) L. Carlucci, G. Ciani, D. M. Proserpio and S. Rizzato, *New J. Chem.*, 2003, **27**, 483.
- 21 Cambridge Structural Database, version 5.35, CCDC, Cambridge, U.K., 2013.
- 22 (a) Q. A. Smith and M. S. Gordon, *J. Phys. Chem. A*, 2011, **115**, 4598; (b) D. B. Ninković, J. M. Andrić and S. D. Zarić, *ChemPhysChem*, 2013, **14**, 237.
- 23 *X-AREA*, version 1.30, program for the acquisition and analysis of data, Stoe & Cie GmbH: Darmstadt, Germany, 2005.
- 24 *X-RED*, version 1.28b, program for data reduction and absorption correction, Stoe & Cie GmbH: Darmstadt, Germany, 2005.
- 25 *X-SHAPE*, version 2.05, program for crystal optimization for numerical absorption correction, Stoe & Cie GmbH: Darmstadt, Germany, 2004.
- 26 G. M. Sheldrick, *SHELX97*, program for crystal structure solution and refinement, University of Göttingen, Göttingen, Germany, 1997.
- 27 *X-STEP32*, version 1.07b, crystallographic package, Stoe & Cie GmbH: Darmstadt, Germany, 2000.
- 28 Mercury 3.3 Supplied with Cambridge Structural Database; CCDC: Cambridge, U.K., 2012.

Influence of N-heteroaromatic $\pi\cdots\pi$ stacking on supramolecular assembly and coordination geometry; Effect of single-atom ligand change

Cite this: DOI: 10.1039/x0xx00000x

Received 00th January ????,
Accepted 00th January ????

DOI: 10.1039/x0xx00000x

www.rsc.org/

Hamid Reza Khavasi* and Bahareh Mir Mohammad Sadegh

In order to understanding of how the polarization of aromatic systems affects the π - π interactions and crystal packing, five Hg(II) complexes, $[\text{HgBr}_2(\text{L}^{2\text{-quin}})_2]_n$, **1**, $[\text{HgI}_2(\text{L}^{2\text{-quin}})]$, **2**, $[\text{HgCl}_2(\text{L}^{3\text{-quin}})]_n$, **3**, $[\text{Hg}_3\text{Br}_6(\text{L}^{3\text{-quin}})_2]_n$, **4**, and $[\text{Hg}_3\text{I}_6(\text{L}^{3\text{-quin}})_2]_n$, **5**, where $\text{L}^{2\text{-quin}}$ and $\text{L}^{3\text{-quin}}$ are *N*-(quinolin-2-yl)pyrazine-2-carboxamide and *N*-(quinolin-3-yl)pyrazine-2-carboxamide ligands have been synthesized and characterized. In comparison to homologues complexes containing *N*-(naphthalene-2-yl)pyrazine-2-carboxamide ligand, $\text{L}^{2\text{-naph}}$, interestingly, structural analysis clearly shows that the replacement of the naphthyl CH group with a nitrogen atom and changing the spatial extent of the π -electron cloud, the propensity of the formation of $\pi\cdots\pi$ interactions increases.

